

SUSTAINED STIMULUS PARADIGMS AND SEXUAL DIMORPHISM OF THE  
AORTIC BAROREFLEX IN RAT

A Thesis

Submitted to the Faculty

of

Purdue University

by

Landan M. Mintch

In Partial Fulfillment of the

Requirements for the Degree

of

Masters of Science in Biomedical Engineering

May 2019

Purdue University

Indianapolis, Indiana

**THE PURDUE UNIVERSITY GRADUATE SCHOOL**  
**STATEMENT OF THESIS APPROVAL**

Dr. John Schild, Chair

Department of Biomedical Engineering

Dr. Ken Yoshida

Department of Biomedical Engineering

Dr. Michael Mirro

School of Informatics and Computing

**Approved by:**

Dr. Julie Ji

Head of the Graduate Program

This is dedicated to my mother, Cindy Mintch, and father, Lantz Mintch.

## TABLE OF CONTENTS

	Page
LIST OF TABLES . . . . .	vii
LIST OF FIGURES . . . . .	viii
LIST OF ABBREVIATIONS . . . . .	xii
ABSTRACT . . . . .	xiv
1 INTRODUCTION . . . . .	1
1.1 Historical Significance and Overview of the System . . . . .	1
1.1.1 High Blood Pressure . . . . .	1
1.1.2 Autonomic Control . . . . .	2
1.1.3 Circulatory Control . . . . .	4
1.1.4 Neurocirculatory Control . . . . .	5
1.1.5 The Baroreflex . . . . .	8
1.2 The Autonomic Nervous System . . . . .	10
1.3 The Baroreflex as a Neural Controller . . . . .	11
1.3.1 Component Parts . . . . .	12
1.3.2 Sexual Dimorphism . . . . .	14
1.3.3 Central Integration . . . . .	15
1.4 Evidence of Resetting in Baroreceptor Function . . . . .	16
1.4.1 Peripheral Resetting . . . . .	17
1.4.2 Central Resetting . . . . .	18
1.5 Clinical Aspects Related to Baroreflex Function . . . . .	19
1.5.1 Baroreflex Activation Therapy . . . . .	19
1.6 Thesis Aims . . . . .	20
2 MATERIALS AND METHODS . . . . .	21
2.1 Introduction . . . . .	21

	Page
2.2 Anesthetic . . . . .	22
2.3 Animal Preparation . . . . .	23
2.4 Surgical Preparation . . . . .	23
2.4.1 Catheterization . . . . .	23
2.4.2 Tracheotomy . . . . .	25
2.4.3 Aortic Depressor Nerve Identification . . . . .	25
2.5 Baroreflex Protocol . . . . .	27
2.5.1 Stimulation Paradigms . . . . .	28
2.6 Data Acquisition and Recording . . . . .	29
2.7 Euthanasia . . . . .	30
2.8 Data Analysis . . . . .	31
2.8.1 Calculations . . . . .	36
2.9 Timeline of Experiment . . . . .	37
3 RESULTS . . . . .	40
3.1 Introduction . . . . .	40
3.2 Research Aims . . . . .	41
3.3 Aim 1: Verifying Acute Baroreflex Dynamics . . . . .	41
3.3.1 Blood Pressure Changes . . . . .	42
3.3.2 Heart Rate Changes . . . . .	45
3.3.3 Timing Characteristics . . . . .	47
3.4 Aim 2: Sustained Baroreflex Dynamics . . . . .	49
3.4.1 Comparison of Peak Depressor Response Dynamics . . . . .	50
3.4.2 Differences in Steady State Depressor and Recovery Responses: Blood Pressure . . . . .	54
3.4.3 Differences in Steady State Depressor and Recovery Responses: Heart Rate . . . . .	61
4 DISCUSSION . . . . .	63
4.1 General Conclusions . . . . .	63
4.2 Specific Conclusions . . . . .	64

	Page
4.2.1 Aim 1 . . . . .	64
4.2.2 Aim 2 . . . . .	66
4.3 Additional Areas to Explore . . . . .	70
4.4 Conclusion . . . . .	70
LIST OF REFERENCES . . . . .	71

## LIST OF TABLES

Table	Page
2.1 Typical Timeline for Experimental Preparation. . . . .	39
3.1 Monoexponential fit following stimulation termination: Averaged values for the variables a, b, and c as well as averaged r squared value in the 10 second monoexponential fit following termination of stimulation at t=600 seconds. . . . .	59

## LIST OF FIGURES

Figure	Page
1.1 American Heart Association guidelines for blood pressure categories [2]. .	2
1.2 Relative feedback gain of different cardiovascular control systems given an acute change in pressure. . . . .	3
1.3 Generic Block diagram illustrating autonomic closed-loop control of effector organs. Homeostatic set point and afferent sensory fiber feedback provide CNS with information for integration and subsequent efferent autonomic outflow via efferent motor fibers. Intermediate control elements can assist in providing effector organ (plant) with proper directions for output (function). . . . .	4
1.4 Simplified BRx Circuit arterial baroreceptors located in aortic arch and carotid sinus activate when artery expansion occurs as a result of rises in BP. Baroreceptor afferent fibers provide feedback to nucleus of solitary tract (NTS) where sympathetic and parasympathetic pathways of BRx are initiated. CVLM, caudal ventrolateral medulla; RVLM, rostral ventrolateral medulla; IML, intermediolateral; NA, nucleus ambiguous; IX, glossopharyngeal nerve; X, vagus nerve [13]. . . . .	8
1.5 Typical changes in carotid sinus nerve activity, heart rate, contractility, and vasoconstriction given different pressure inputs [20]. . . . .	11
1.6 Blood pressure regulation system overview. CNS, central nervous system; SA, sinoatrial node; RRI, R peak to R peak interval; SV, stroke volume; CO, cardiac output. . . . .	12
1.7 Pressure-IFF relationship recorded from rat aortic BRs. Discharge frequency of A-type myelinated axons generally more robust and regular with higher firing frequency. In contrast, discharge frequency from C-type unmyelinated axon lower and more variable [23]. . . . .	13
1.8 Prevalence of HBP in adults $\geq 20$ years of age by sex and age [1]. . . . .	15
1.9 Major connections of supramedullary sites within the medulla. Emphasis put on the NTS and other major autonomic brain regions. Caudal ventrolateral medulla (CVLM), dorsal motor nucleus of the vagus (DVN), nucleus ambiguous (NA), and rostral ventrolateral medulla (RVLM) [7]. .	16

Figure	Page
1.10 Resetting of BRs in response to elevations in pressure. A) quick, b) acute, c) chronic [30]. . . . .	18
2.1 Arrangement of components to monitor pressure in the femoral artery: 1) 5 mL syringe of heparinized (30 U/m) saline, 2) calibrated pressure transducer, 3) T-split luer lock, 4) PE-100 catheter. . . . .	24
2.2 Tracheostomy with tracheal catheter, trachea, and suture knot labeled. . . . .	26
2.3 Vagus Nerve (CNX), aortic depressor nerve (ADN), Platinum-Iridium hook, and central carotid artery. . . . .	27
2.4 A 2-s snapshot illustrating the difference between continuous and burst pulse trains, IBI = inter-burst interval in milliseconds (ms). . . . .	30
2.5 Typical depressor response (bottom) with segmented baseline A (A - orange) and baseline B (B - green). Average for baseline A and B were 102.69 and 48.49 mmHg, respectively. . . . .	33
2.6 Typical 2V 50 Hz acute depressor response with associated blood pressure (top), raw ECG (middle), and converted heart rate in beats per minute (bottom). Rapid reduction in pressure and heart rate was seen following stimulation (vertical black line) of ADN until stimulation end (red vertical line) allowed recovery. BASELINE A (orange) 10 seconds of pressure prior to stimulation onset. BASELINE B (green) 1 second of pressure about the peak depressor response. . . . .	34
2.7 Typical 2V 5 Hz sustained depressor response (middle). Small 2-s epoch of beat to beat blood pressure (top). A rapid reduction in pressure was seen following stimulation (black vertical line) of ADN until stimulation end (red vertical line) allowed recovery. Associated epochs (bottom) were segmented and plotted. BASELINE X (cyan) 30 seconds of pressure prior to stimulation onset. BASELINE Y (gold) 30 second of pressure taken just prior to end of stimulation. BASELINE Z (magenta) 30 seconds of pressure taken 30 seconds after the end of stimulation. . . . .	35
3.1 Low threshold myelinated afferents in female rats elicit the BRx at lower stimulation frequencies than in male rats. In situ, bipolar stimulation of the left ADN at standard 2V. Stimulation onset elicited a rapid fall in BP albeit with differences across the response from male (A) and female (B) rats. Each trial consisted of a non-fixed duration of stimulation at randomly selected frequencies maintained only until there was a clear indication of a minimum in the depressor response. Runs are arranged here in ascending order, with a green dashed line indicating stimulation start at $t = 10$ seconds. . . . .	43

Figure	Page
3.2 The BRx in female rats elicits a greater depressor response at low rates of 2V bipolar stimulation of the left ADN than in male rates. Average % changes in MAP evoked through bipolar stimulation of the left ADN using randomly selected frequencies (1 to 50 Hz) at a regulated 2V amplitude. Data are means $\pm$ SD, # p <0.01. . . . .	44
3.3 The BRx in female rats elicits a greater change in heart rate at rates of 2V bipolar stimulation of the left ADN than in male rates. Average changes in the Baseline B HR evoked through bipolar stimulation of the left ADN using randomly selected frequencies (1 to 50 Hz) at a regulated 2V amplitude. Dotted lines denote the average resting HR prior to stimulation onset. Data are means $\pm$ SD, * p <0.05 and # p <0.01. . . . .	46
3.4 Acute time to peak fall in blood pressure response following the onset of acute stimulation differs between male and female rats. Average time to peak (TTP) in seconds for randomly selected stimulation frequencies (1-50 Hz). Data are not present for male response in frequencies 1, 2, and 5 Hz due to there being no depressor response present. Data are means $\pm$ SD.	48
3.5 Percent change in mean arterial pressure between baseline A and baseline B following the onset of 2 Hz stimulation differs between male and female rats. Average percent change in blood pressure (dMAP) for acute (A), continuous (B), and burst (C) paradigms. Data are means $\pm$ SD. . . . .	50
3.6 Percent change in mean arterial pressure between baseline A and baseline B following the onset of 5 Hz stimulation differs between male and female rats. Average percent change in blood pressure (dMAP) for acute (A), continuous (B), and burst (C) paradigms. Data are means $\pm$ SD. . . . .	51
3.7 Percent change in mean arterial pressure between baseline A and baseline B following the onset of 5 Hz stimulation differs between male and female rats. Average percent change in blood pressure (dMAP) for acute (A), continuous (B), and burst (C) paradigms. Data are means $\pm$ SD. . . . .	52
3.8 Percent change in mean arterial pressure between baseline A and baseline B following the onset of 5 Hz stimulation differs between male and female rats. Average percent change in blood pressure (dMAP) for acute (A), continuous (B), and burst (C) paradigms. Data are means $\pm$ SD. . . . .	53
3.9 The BRx in female rats elicits a greater residual depressor response at the end of a 600 second continuous stimulation of the left ADN than in the male rats. Average % changes in dMAP evoked through bipolar stimulation of the left ADN using randomly selected frequencies (2 and 5 Hz) at a regulated 2V amplitude. Data are means $\pm$ SD, * p <0.05. . . . .	55

Figure	Page
3.10 The recovery of dMAP (baseline X vs baseline Z) following termination of continuous bipolar stimulation of the left ADN is different between male and female rats. Average % changes in dMAP evoked through bipolar stimulation of the left ADN using randomly selected frequencies (2 and 5 Hz) at a regulated 2V amplitude. Data are means $\pm$ SD, * p <0.05. . . .	56
3.11 The BRx in female rats elicits a greater depressor response at the end of a 600 second burst stimulation of the left ADN than in the male rats. Average % changes in dMAP evoked through bipolar stimulation of the left ADN using randomly selected frequencies (2 and 5 Hz) at a regulated 2V amplitude. Data are means $\pm$ SD, * p <0.05. . . . .	57
3.12 The recovery of dMAP following termination of burst bipolar stimulation of the left ADN is different between male and female rats. Average % changes in dMAP evoked through bipolar stimulation of the left ADN using randomly selected frequencies (2 and 5 Hz) at a regulated 2V amplitude. Data are means $\pm$ SD, * p <0.05. . . . .	58
3.13 Example of an ideal exponential fit for the 10 seconds of recovery following stimulation termination at t= 774.34 seconds. Filtered BP in blue, the 10 seconds of BP following stimulation termination in green, and an exponential fit with coefficients a=102.95 b=21.296 and c=0.1551 with r squared value = 0.9659. . . . .	60
3.14 Average change in BPM between baselines X, Y, and Z at sustained 2 Hz stimulation. Male (blue) had higher average resting BPM than female (orange). Continuous stimulation is denoted by circles and burst stimulation by triangles. Average change in BPM between baselines is denoted numerically between data points. Data are mean $\pm$ SD. . . . .	61
3.15 Average change in BPM between baselines X, Y, and Z at sustained 5 Hz stimulation. Male (blue) had higher average resting BPM than female (orange). Continuous stimulation is denoted by circles and burst stimulation by triangles. Average change in BPM between baselines is denoted numerically between data points. Data are mean $\pm$ SD. . . . .	62

## LIST OF ABBREVIATIONS

CVD	Cardiovascular Disease
HPB	High Blood Pressure
AHA	American Heart Association
ANS	Autonomic Nervous System
CNS	Central Nervous System
PNS	Peripheral Nervous System
HR	Heart Rate
BP	Blood Pressure
BPM	Beats Per Minute
CO	Cardiac Output
SV	Stroke Volume
TPR	Total Peripheral Resistance
ACh	Acetylcholine
NA	Nucleus Ambiguus
NTS	Nucleus of the Solitary Tract
BRx	Baroreflex
SCI	Spinal Cord Injury
IFF	Instantaneous Firing Frequency
ADN	Aortic Depressor Nerve
CVLM	Caudal Ventrolateral Medulla
RVLM	Rostral Ventrolateral Medulla
MAP	Mean Arterial Pressure
IBI	Inter Beat Interval
BAT	Baroreflex Activation Therapy

AP	Action Potential
TTP	Time to Peak
RRI	R to R Interval

## ABSTRACT

Mintch, Landan M. M.S.B.M.E., Purdue University, May 2019. Sustained Stimulus Paradigms and Sexual Dimorphism of the Aortic Baroreflex in Rat. Major Professor: John Schild.

The neurophysiological pathways associated with beat-to-beat regulation of mean arterial pressure are well known. Less known are the control dynamics associated with short term maintained of arterial blood pressure about a homeostatic set point. The baroreflex (BRx), the most rapid and robust of neural reflexes within the autonomic nervous system, is a negative feedback controller that monitors and regulates heart rate and blood pressure. By leveraging the parasympathetic and sympathetic divisions of the autonomic nervous system, the BRx can change blood pressure within a single heart beat. To better understand these controller dynamics, a classic BRx reflexogenic experimental preparation was carried out. This thesis reconfirmed previous observations of an electrically-evoked sexually-dimorphic peak depressor response in the BRx of Sprague-Dawley rats and verified that these functional reflexogenic differences carry over to sustained electrical paradigms. Further, it uncovered interesting recovery dynamics in both blood pressure and heart rate. The rat aortic depressor nerve was used as an experimental target for electrical activation of the parasympathetic-mediated reduction in mean arterial pressure. The duration, frequency, and patterning of stimulation were explored, with emphasis on differences between sexes. By measuring the normalized percent decrease in mean arterial pressure as well as the differences in beats per minute during rest and during stimulation, the null hypothesis was rejected.

## CHAPTER 1. INTRODUCTION

### 1.1 Historical Significance and Overview of the System

#### 1.1.1 High Blood Pressure

The leading cause of death in the United States has long been and continues to be cardiovascular disease (CVD) [1]. Prevention strategies for CVD include healthy eating, regular physical activity, limiting inhalation of smoke, and moderate to no consumption of alcohol. However, even with these widely recognized approaches to mitigating risk factors, the prevalence of CVD has been steadily increasing [2]. In 2016, 17.6 million deaths worldwide were attributed to CVD, an increase of 14.5% from 2006 [1]. It is well recognized that a major contributing factor exacerbating the overall severity of CVD is high blood pressure (HBP, hypertension) [2]. The American Heart Association (AHA) has set guidelines for classifying what is considered normal and abnormal arterial pressures [Figure 1.1]. Clinical interventions become increasingly invasive as pressures increase into more severe levels (Stage 2, or hypertensive crisis) though a hypotensive crisis is also of concern. In a follow up to the 2003-2007 REGARDS (REasons for Geographic And Racial Differences in Stroke) study, 63% of incident CVD events were associated with patients with HBP. In the United States, the percentage of hypertension among age-adjusted adults  $\geq 20$  years of age was estimated to be 46% (49% in males, 42.8% for females) in 2013-2016 [1]. The financial burden for those 116 million Americans is estimated to be around \$55.9 billion (National Health and Nutrition Examination Survey, CDC). The World Health

Organization has estimated HBP is at least one of the root causes in 12.5% of deaths worldwide, supporting the often stated position that hypertension is a silent killer [3].

### 1.1.2 Autonomic Control

The etiology of HBP is inextricably associated with the neural and hormonal mechanisms that underlie the regulation of arterial blood pressure about an equilibrium. Mechanisms that are collectively under the control of the autonomic nervous system (ANS).

BLOOD PRESSURE CATEGORY	SYSTOLIC mm Hg (upper number)		DIASTOLIC mm Hg (lower number)
NORMAL	LESS THAN 120	and	LESS THAN 80
ELEVATED	120 – 129	and	LESS THAN 80
HIGH BLOOD PRESSURE (HYPERTENSION) STAGE 1	130 – 139	or	80 – 89
HIGH BLOOD PRESSURE (HYPERTENSION) STAGE 2	140 OR HIGHER	or	90 OR HIGHER
<b>HYPERTENSIVE CRISIS</b> (consult your doctor immediately)	HIGHER THAN 180	and/or	HIGHER THAN 120

Fig. 1.1: American Heart Association guidelines for blood pressure categories [2].

The ANS monitors and controls homeostatic variables by way of central (CNS) and peripheral (PNS) nervous system pathways. Homeostasis, the proclivity towards internal stability or equilibrium of systems within an organism, is especially important for physiological processes such as blood pressure and heart rate regulation. CNS control systems rely upon feedback pathways via fast neurogenic mechanisms, intermediate hormonal mechanisms, and slow intrinsic mechanisms [4] [Figure 1.2]. Hormonal mechanisms, such as those regulating fluid and salt balance by the kidneys, most often occur over the course of several minutes to days or longer [5]. In contrast, acute neural mechanisms most often respond on a time scale of seconds to

minutes, although evidence exists supporting long term regulation of BP [6]. The experimental objectives of this thesis are constrained to short term, acute responses where autonomic homeostasis can be carefully monitored and maintained throughout the experimental protocol.

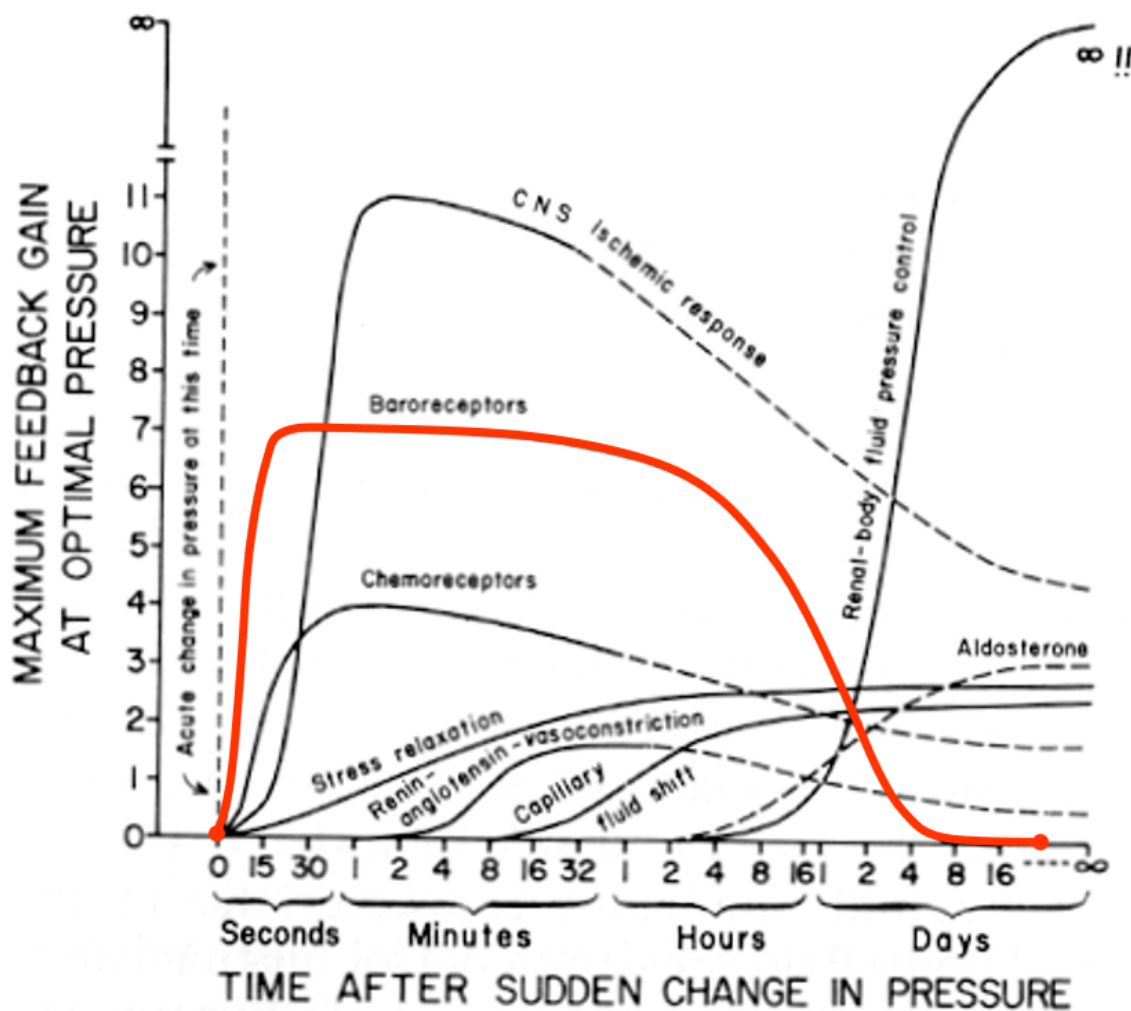


Fig. 1.2: Relative feedback gain of different cardiovascular control systems given an acute change in pressure.

### 1.1.3 Circulatory Control

The ANS is an integrated network of reflexes composed of sensory and motor nerve fibers that make possible the closed loop negative-feedback control of central regulatory networks [7]. Autonomic sensory fibers arise from cell bodies in dorsal root and cranial nerve ganglia and are responsible for transduction and translation of the control variable into an information stream that can be interpreted by the CNS. The difference between the homeostatic balance (in this case a pressure set point) and the feedback from these sensors allow summation and integration at the level of the brainstem and higher centers within the CNS and subsequent autonomic efferent drive via motor fibers to effector organs (plant) [Figure 1.3]. The regulatory set point and compensatory efferent drive are often a consequence of the interaction between multiple control centers and pathways associated with the ANS including the nucleus of the solitary tract, the nucleus ambiguus, and the hypothalamus.

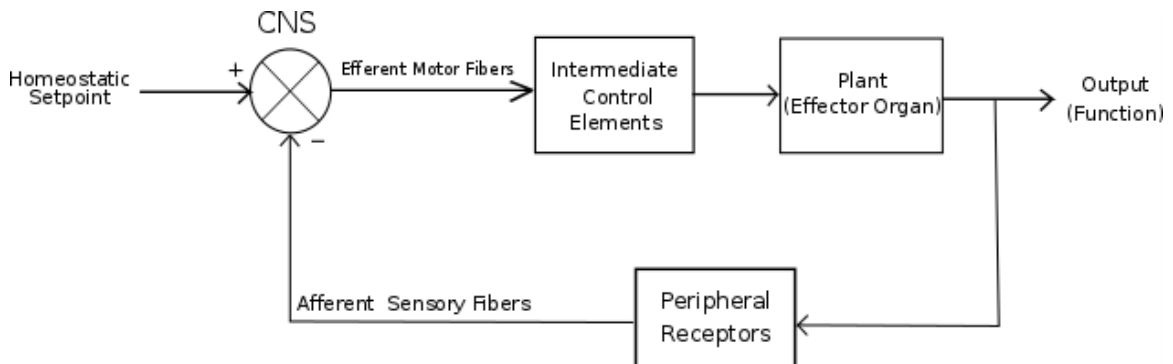


Fig. 1.3: Generic Block diagram illustrating autonomic closed-loop control of effector organs. Homeostatic set point and afferent sensory fiber feedback provide CNS with information for integration and subsequent efferent autonomic outflow via efferent motor fibers. Intermediate control elements can assist in providing effector organ (plant) with proper directions for output (function).

The ANS maintains heart rate (HR) and blood pressure (BP) within an operating range (human: mean arterial BP (MAP): 100 +/- 20 mmHg; normal sinus-rhythm HR: 60 beats per minute [bpm]). In response to physiological demands upon the circulatory system, these ranges can differ substantially (tachycardia:  $\geq 100$  bpm; bradycardia:  $\leq 60$  bpm). Beat-to-beat neurocirculatory control broadly involves the regulation of 5 general control variables: cardiac output (CO), stroke volume (SV), HR, BP, and total peripheral resistance (TPR). CO, or the volume per unit time of pumped blood, is a function of SV and HR:

$$CO = SV * HR \quad (1.1)$$

And is also a measure of cardiac workload in that the heart must maintain mean arterial pressure (MAP) about a resistance to circulatory flow:

$$CO = \frac{MAP}{TPR} \quad (1.2)$$

Therefore, MAP is highly dependent upon SV, HR, and TPR:

$$MAP = (SV * HR) * TPR \quad (1.3)$$

#### 1.1.4 Neurocirculatory Control

Two distinct functional divisions of the ANS assist in its control over HR and BP: the parasympathetic and sympathetic nervous systems. A third division, the enteric nervous system, largely regulates gastrointestinal secretion and motility and can be considered a separate division of the ANS and not directly relevant to the scope of this thesis [7]. The sympathetic nervous system regulates the use of metabolic resources and coordinating the emergency responses of the body to potentially life threatening situations (fight or flight) while the parasympathetic presides over the restoration of metabolic reserves and the elimination of wastes (rest and digest) [5]. The competitive interactions between the sympathetic and peripheral nervous systems has long been

termed sympathovagal balance. This competitive interaction functions much as an adjustable fulcrum i.e. there most often exists a reciprocal relationship between sympathetic and parasympathetic drive. Sympathovagal balance has been widely recognized as a critically important factor in responding to decreases or increases in BP about the set point, especially as it pertains to hypotension and hypertension, respectively [8].

Neural communication within these systems differ with respect to neurotransmitters and receptors. Cholinergic receptors (acetylcholine) are utilized in both divisions while adrenergic receptors (catecholamines) are almost exclusively located in the sympathetic division [5]. Differences in neuroanatomical organization are more distinct. Autonomic efferent pathways incorporate two distinct cell bodies: one a preganglionic (from CNS to ganglion) and the other postganglionic (from ganglion to effector organ) neuron [5]. Sympathetic preganglionic neurons originate from the intermediolateral cell column of the spinal cord, the major caudal nervous tissue of the CNS. These short neurons begin at varying levels of thoracic and lumbar sections (T1 L2) of the spinal cord and exit via ventral spinal rootlets [7]. The neurotransmitters responsible for communication within the sympathetic system are largely cholinergic for the presynaptic neurons and largely adrenergic for the postsynaptic neurons, albeit with some exceptions such as sweat glands [7].

Unlike the sympathetic nervous system, both pre- and post-ganglionic fibers of the parasympathetic mainly involve cholinergic receptors. Though acetylcholine (ACh) is not the only neurotransmitter, it is the most abundant. Parasympathetic preganglionic neurons lie in the cranial (CIII, CVII, CIX, CX) and sacral (S2- S4) portions of the spinal cord. Preganglionic neurons begin in the medulla oblongata: specifically the dorsal vagal nucleus and nucleus ambiguus. Preganglionic fibers of the parasympathetic are much longer than those of the sympathetic and can travel as far as to the end organs or ganglia embedded near them. The third cranial nerve is responsible for oculomotor function; the seventh cranial is responsible for facial innervation; the ninth cranial (glossopharyngeal) innervates the tonsils, pharynx, middle ear, and

parts of the tongue; and the tenth cranial, which will be the focus of the majority of this work, is the vagus nerve. The vagus is important in parasympathetic control of the heart, viscera of the neck, thorax, and gastrointestinal system [9].

Fiber pathways of the vagus emerge or converge onto four nuclei of the medulla of which the nucleus ambiguus and dorsal motor nucleus are primarily concerned with efferent outflow while the solitary nucleus is concerned with afferent projections [10]. The nucleus ambiguus (NA) is a CNS structure vital for cardiovascular regulation. Cholinergic preganglionic parasympathetic motor neurons (efferent transmission) of the external formation of the NA project directly to the heart [11]. Parasympathetic efferent outflow originating from the dorsal motor nucleus of the vagus nerves and NA decrease cardiac activity in response to rapid increases in BP [12]. Afferent pathways begin at end organ sensors and project to the main CNS site within the medulla: the nucleus of the solitary tract (NTS). One of the fastest and most robust neural reflexes in the ANS, the baroreceptor reflex (baroreflex, BRx) regulates HR, SV and TPR via the vagus nerve and cardiac sympathetic nerves to stabilize BP [5] [Figure 1.4].

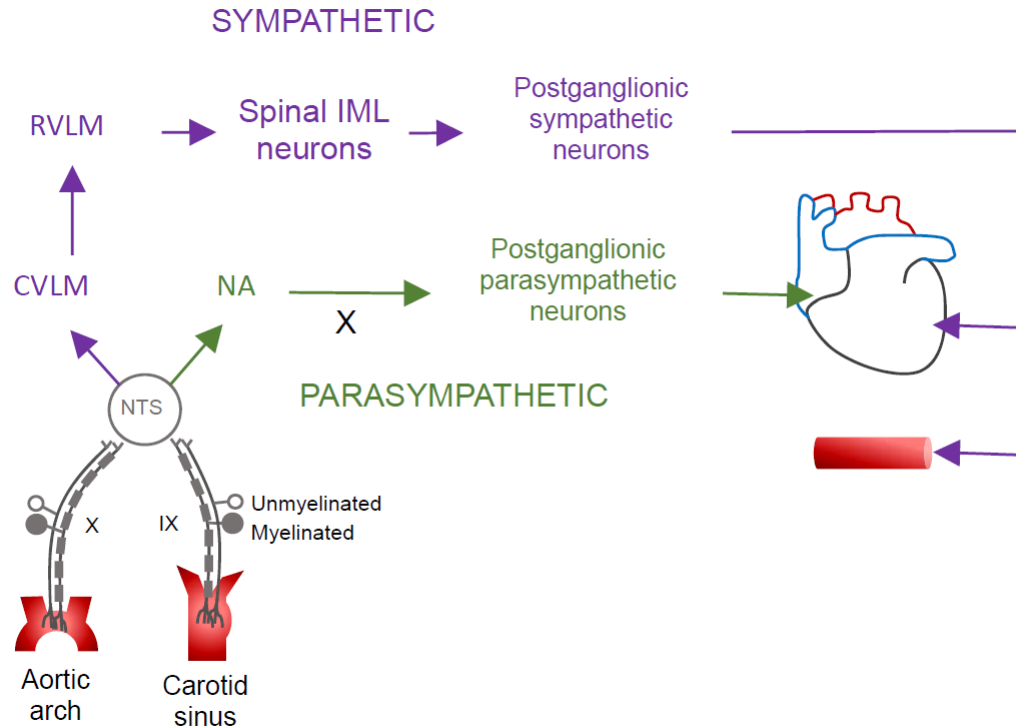


Fig. 1.4: Simplified BRx Circuit arterial baroreceptors located in aortic arch and carotid sinus activate when artery expansion occurs as a result of rises in BP. Baroreceptor afferent fibers provide feedback to nucleus of solitary tract (NTS) where sympathetic and parasympathetic pathways of BRx are initiated. CVLM, caudal ventrolateral medulla; RVLN, rostral ventrolateral medulla; IML, intermediolateral; NA, nucleus ambiguus; IX, glossopharyngeal nerve; X, vagus nerve [13].

### 1.1.5 The Baroreflex

The BRx is a negative feedback controller responsible for maintaining homeostatic and dynamic control of the cardiovascular system [14]. The BRx control system, as with all closed loop control systems, consists of sensors, an integrator, and an effector [Figure 1.4]. Baroreceptor (BR) terminal endings are the sensors in the aortic arch and carotid sinus that encode vessel stretch [15]. Increasing pressure in these arteries

stretches the walls and excites BRs, increasing their firing rate of action potentials (AP). The threshold pressure required to excite BRs differs depending on fiber type which are generally classified as either low threshold (A-type, myelinated) or high threshold (C-type, unmyelinated) [16]. APs travel towards the CNS integrator, the nucleus of the solitary tract (NTS). Since the BRx appeals to both the sympathetic and parasympathetic divisions, it is the job of the NTS to integrate afferent feedback and assess the relative magnitude of sympathovagal drive. Parasympathetic drive is an order of magnitude faster allowing the BRx controller to reduce BP in a single cardiac cycle [5]. Parasympathetic efferent drive directly slows the pacing cells of the effector - the heart - resulting in a decrease in HR and subsequent decrease in BP and CO.

This thesis will investigate the BRx neural control on HR and BP through selective activation of BR fibers. An experimental paradigm was established to control homeostatic condition and apply perturbations to the BRx controller with emphasis on differences between sexes. Perturbations include interrogation of BRx pathways through direct electrical activation of BR afferents in rat. Better understanding the sympathovagal balance in long-term neural control of BP and HR could provide an interesting clinical target for electrical therapies. Historically, pharmacological interventions have proved helpful, yet 15% of patients still experience symptoms of HBP (resistant hypertension) [17]. Often referred to as bioelectric therapies, these new electrical interventions could potentially provide targeted intervention by preferentially tapping into the neurocirculatory arms commonly associated with hypertension and other CVD related comorbidities.

## 1.2 The Autonomic Nervous System

The ANS maintains homeostatic set points through a network of interdependent reflexes. Cardiovascular reflexes such as the baroreceptor, chemoreceptor, and atrial receptor reflex rely on information encoded by sensors in the periphery. Some of the stimuli these sensors encode include pressure, fluid volume, and chemical substances. Efferent neural drive can cause HR, SV, CO, TPR, and fluid balance changes based off sensor feedback. Less appreciated is that these homeostatic variables can also be affected by afferent modulation/manipulation. Other regulatory networks such as the orthostatic reflex, integrate the information from a variety of physiological sensors. Postural changes result in large shift of blood volume, changing the discharge characteristics of afferent arterial baroreceptors, chemoreceptors, and atrial receptors. The orthostatic reflex can drive competitive interactions between the parasympathetic and sympathetic limbs to maintain proper tissue perfusion [4]. Insufficient orthostatic control, termed orthostatic intolerance, is a complication marked by frequent bouts of syncope, or loss of consciousness. Furthermore, more wide spread autonomic dysfunction can arise from damage to any one part of control systems including sensors, conduction pathways or central networks. Common causes of autonomic disorders include diabetes, aging, Parkinsons disease, and spinal cord injury (SCI) [18, 19].

### 1.3 The Baroreflex as a Neural Controller

The BRx is a negative feedback controller that maintains acute, i.e. beat-to-beat control of BP by way of parasympathetic control of HR and sympathetic control of TPR and SV [15]. The quick decrease in elevated BP following BR activation is among the fastest and most robust reflexes in the body and facilitated by a decrease in HR (bradycardia) and an increase in peripheral vasodilation. The high gain and quick response of the BRx allows HR and BP regulation within a single heartbeat [13]. In instances of lowered pressure, the reciprocal occurs, with an increase in TPR and SV via sympathetic nerves and increase in HR (tachycardia) via parasympathetic inhibition [Figure 1.5].

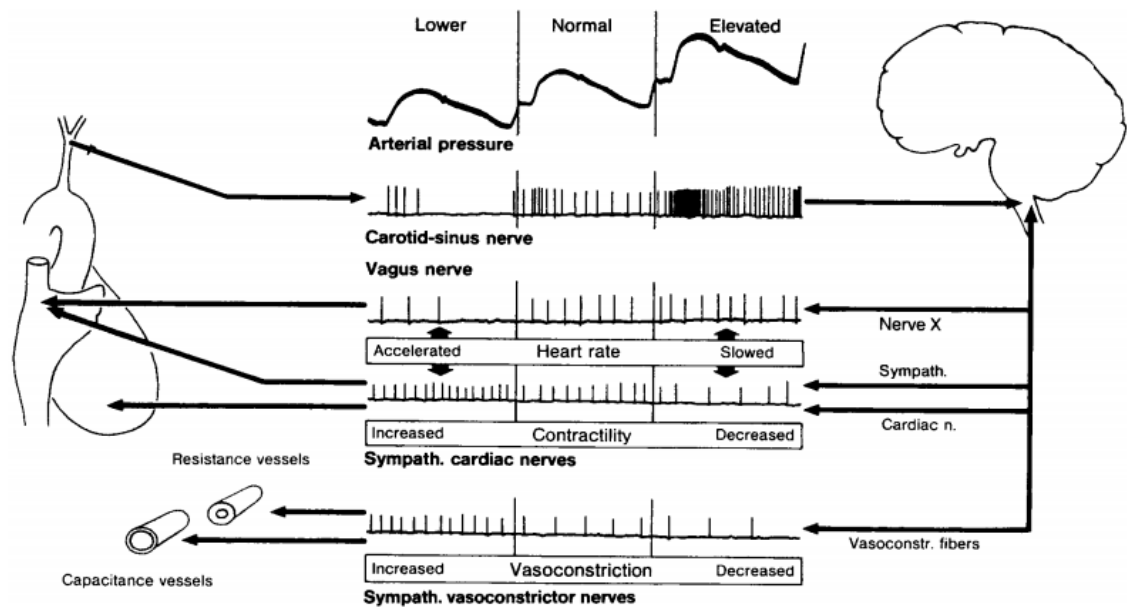


Fig. 1.5: Typical changes in carotid sinus nerve activity, heart rate, contractility, and vasoconstriction given different pressure inputs [20].

### 1.3.1 Component Parts

Wehrwein et al. summarized the component parts of the BRx to include MAP, mechanosensory transduction, afferent pathways, central neural circuits, efferent pathways, receptor pharmacology, integration with other key homeostatic inputs, molecular biology, and/or other elements [15] [Figure 1.6].

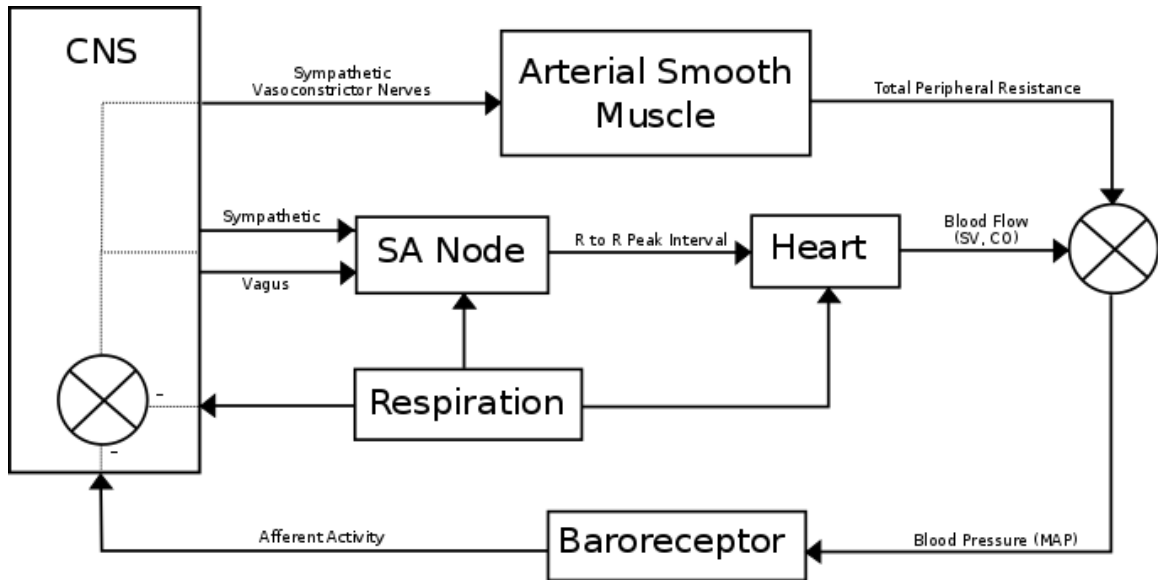


Fig. 1.6: Blood pressure regulation system overview. CNS, central nervous system; SA, sinoatrial node; RRI, R peak to R peak interval; SV, stroke volume; CO, cardiac output.

BR terminal endings transduce and neurally encode the magnitude and time course of BP into patterns of action potential (AP) discharge [21]. When pressure is elevated, artery lumen expands, causing the stretch-sensitive BRs to fire APs along the length of the BRs. Large diameter, A-type BRs activate at BPs between 30-90 mmHg in contrast to small diameter, C-type BRs which have thresholds of activation in the range of 70-140 mmHg [5]. Within their physiological operating range, BRs respond to a steady stretch with a steady (and potentially deterministic) discharge which increases in frequency as the stretch is increased, with strong sensitivity to the

rate of change of the stimulus [22]. Instantaneous firing frequency (IFF), defined as the inverse of time between neighboring AP spikes, assists in illustrating the different neural encoding of these BR fiber types. The pressure-discharge relationship differs greatly, with A type fibers firing at lower pressures thresholds and with less variability in their IFF than their C-type cousins [23]. This threshold-firing relationship defines the dynamic range of these sensors [Figure 1.7].

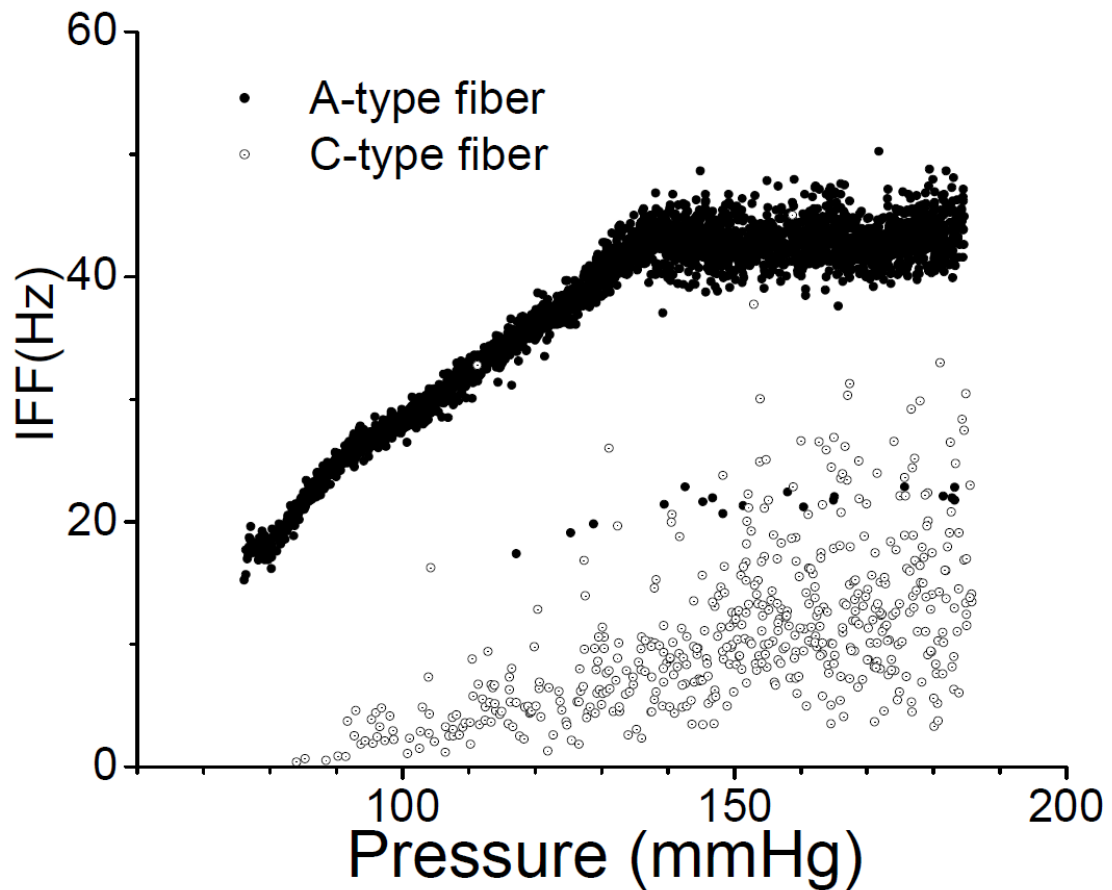


Fig. 1.7: Pressure-IFF relationship recorded from rat aortic BRs. Discharge frequency of A-type myelinated axons generally more robust and regular with higher firing frequency. In contrast, discharge frequency from C-type unmyelinated axon lower and more variable [23].

APs travel towards the CNS through myelinated (A-type) and unmyelinated (C-type) BRs [15]. The large body of science related to BR function is concerned with fast-propagating ( $\geq 10$  m/s) A-type BRs as slow-propagating ( $\leq 2$  m/s) C-type are much smaller and therefore increasingly difficult to study (2-10 micrometers versus  $< 2$  micrometers, respectively) [24]. A-type BRs can be activated at much lower voltages than C-type BRs [25–27].

### 1.3.2 Sexual Dimorphism

Previous work in our lab has identified a 2nd phenotype of myelinated BR afferent, termed Ah. Ah phenotype has many of the nonoverlapping electrophysiological properties and chemical sensitivities of both myelinated A-type and unmyelinated C-type BR afferents [25]. Selective activation of aortic depressor nerve (ADN) myelinated fibers using low-voltage, low-frequency stimulation evoked a BRx-mediated depressor response 3-7 times greater in female than male rats [25]. The relative subset of vagal sensory neurons make up over 50% of myelinated BRs in female rats but less than 2% in age matched males [13]. This sex-related difference in autonomic control may potentially provide some insight into the differing prevalences of hypertension between males and females [Figure 1.8].

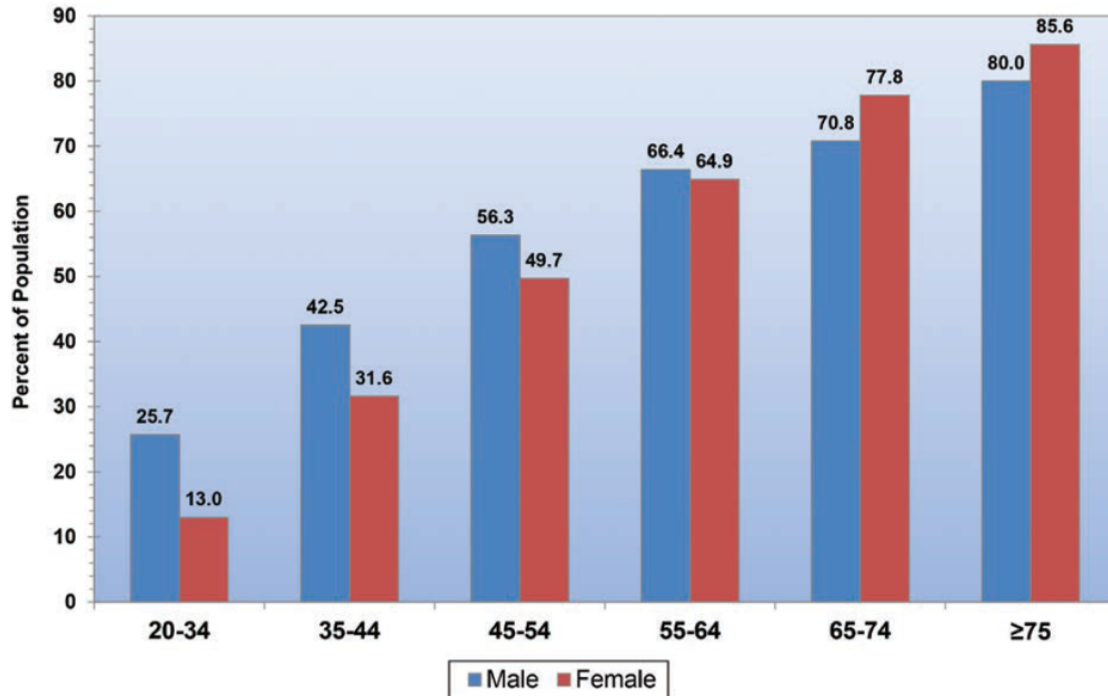


Fig. 1.8: Prevalence of HBP in adults  $\geq 20$  years of age by sex and age [1].

### 1.3.3 Central Integration

Regardless of fiber-type activated, BR excitation causes a volley of afferent APs towards the CNS. This information travels along afferent myelinated and unmyelinated axons to CNS integrators like the NTS. The NTS is one of the main relay stations within the CNS for afferent transmission of viscerosensory information [28]. The NTS receives moment-to-moment updates about the status of respiration, gastrointestinal, and most importantly cardiovascular function. This information can then be used to change the reflex response of the BRx. The manner in which the NTS relays this information onward to higher CNS structures depends to a large extent upon which arm of the ANS is being preferentially activated. Primary parasympathetic inputs (the first to arrive) will synapse at the NTS and make connections with the dorsal motor nucleus of the vagus (DMN) and nucleus ambiguus (NA) before moving along to the cervical vagus. Primary sympathetic inputs will synapse at the NTS and then

project to either the caudal ventrolateral medulla (CVLM) or rostral ventrolateral medulla (RVLM) before leaving to the spinal cord and viscera [Figure 1.9].

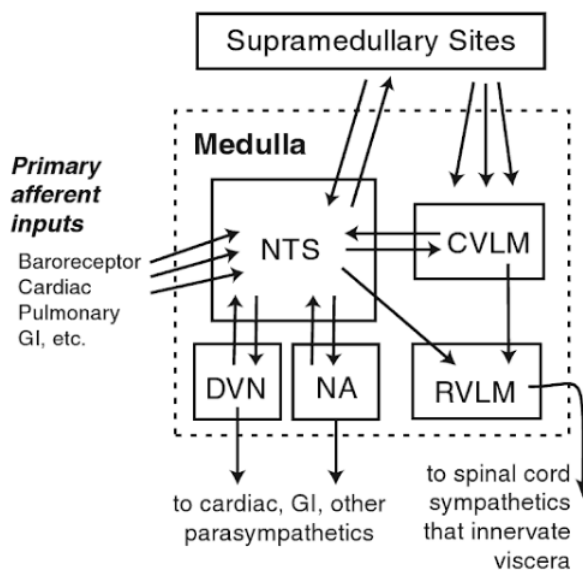


Fig. 1.9: Major connections of supramedullary sites within the medulla. Emphasis put on the NTS and other major autonomic brain regions. Caudal ventrolateral medulla (CVLM), dorsal motor nucleus of the vagus (DVN), nucleus ambiguus (NA), and rostral ventrolateral medulla (RVLM) [7].

#### 1.4 Evidence of Resetting in Baroreceptor Function

In addition to differences in BR anatomy, there has been a large body of research associated with changes in BR firing given different conditioning pressures. Normal human physiology experiences a wide range of steady state pressures both elevated and below normal MAP. If the sensors simply linearly encoded pressure, the limited operating range could cause saturation or silence, resulting in hindered cardiovascular homeostasis. For example, in exercise, where MAP can reach 150 mmHg, nearly all of the A type BRs would be saturated [Figure 1.7]. To deal with this, the ANS establishes a new set point for arterial BP shifting the dynamic range of BRs and

modifying the sensitivity or gain of the BRx. Termed resetting, BRs can have characteristically different thresholds for activation given sustained exposure to differing MAP. Acute resetting can occur during brief elevated pressure while chronic resetting can be found in BRs of hypertensive animals or those with distinct structural changes of the vessels that BR terminals innervate [29]. Resetting is a potential hypothesis to explain the underlying mechanism of hypertension. Hypertension is caused by an imbalance of sympathetic and parasympathetic cardiovascular regulation [30].

Resetting can happen at the BRs (peripheral resetting) or at the level of the CNS (central resetting) [28]. Both peripheral and central resetting result in differences in BRx efferent drive though the mechanisms underlying these changes may differ substantially. Often, the threshold for BR activation is used to help quantify the amount of resetting. The threshold pressure is found by assessing when a certain number of afferent spikes are recorded (BR activity). The response curve are often sigmodal in shape with an asymptotic region at high BR activity indicating the upper limit of BR activity [Figure 1.10]. This quantification of activity to pressure represents the dynamic range of BRs while the slope of the line represents the gain.

#### 1.4.1 Peripheral Resetting

Peripheral resetting at the BR can occur through three mechanisms: (1) changes in the mechanical properties of the vessel wall (changing strain seen at BR terminal endings); (2) ionic mechanisms operating at the level of the membrane (activation of Na, K, -ATPase), (3) substances released from the endothelium during vascular stretch [30]. These mechanisms can affect the type of peripheral resetting which is generally classified based off the duration of onset. In instantaneous peripheral resetting, the differences in pressures between systole and diastole are so great that nerve activity is reduced during the diastolic phase. Acute peripheral resetting can begin in as little as a few minutes following a change in MAP. Stabilization can occur anywhere from 5 to 15 minutes after the initial change [29]. Chronic peripheral

resetting is often seen in hypertension and in atherosclerosis and is associated with sustained inhibition of BR activity [30].

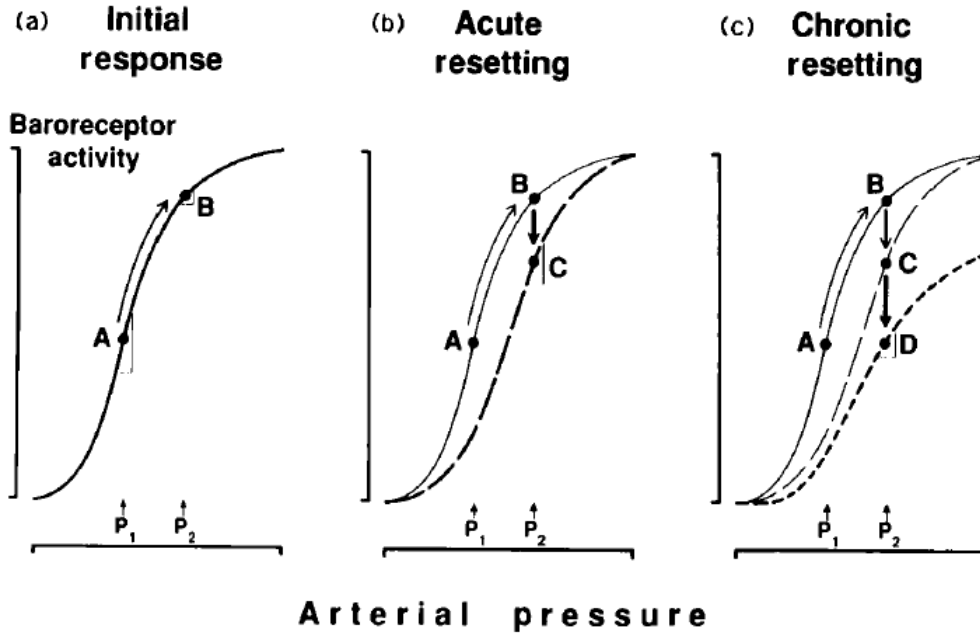


Fig. 1.10: Resetting of BRs in response to elevations in pressure. A) quick, b) acute, c) chronic [30].

#### 1.4.2 Central Resetting

Central resetting or adaptation is the sustained inhibition of efferent sympathetic activity even when afferent BR activity would predict efferent sympathetic activation [31]. Central resetting is most obvious with the lack of pulsatile pressures. It is believed that the pulsatile pressures sensitizes BRs and promotes increased afferent activity. As highlighted by Chapleau et al, central resetting is when efferent sympathetic activity is inappropriately high for a given level of BR activity. Believed to be a result of interactions outside of humoral or neural reflex systems, central resetting involves reduced sensitivity of sympatho-inhibitory neurons driven by BR afferent

activity. In summary, an insufficient and impaired coupling between afferent drive and efferent outflow [31].

## 1.5 Clinical Aspects Related to Baroreflex Function

There is a large body of evidence suggesting decreased autonomic function in patients with diabetes and following SCI [32–34]. While symptoms can span from cardiovascular, to bladder, bowel, musculoskeletal, sexual, behavioral, and temperature regulatory impairment, I will focus on those studies related to cardiovascular impairment. Reduced cardiovascular reflexes, autonomic dysreflexia, and orthostatic hypotension are the main CVD related ailments in SCI patients [32]. Autonomic neuropathy, a common complication of diabetes mellitus, involves the impairment of cardiovascular autonomic control [34]. Baroreflex sensitivity is a useful measure in quantifying the gain of BRx control on HR. Usually reported in ms/mmHg, BRS defines the change in interbeat interval (IBI) in milliseconds per unit change in BP [35]. Much like that of able-bodied, CVD is the leading cause of morbidity and mortality in SCI [33]. SCI patients often live with low resting MAP, intermittent periods of uncontrolled hypertension (autonomic dysreflexia), and hypotensive bouts during postural changes. Some studies discern complications by level of injury (high lesion versus low lesion). In general, high-level lesions exhibit greater baroreflex dysfunction than low-level lesions [33].

### 1.5.1 Baroreflex Activation Therapy

Baroreflex activation therapy or BAT, is a new approach to treating resistant hypertension by eliciting a reflex response to lower BP through electrical stimulation of the carotid sinus BRs. A few clinical studies have already showed efficacy of treatment [36,37]. The devices used in these trials are described below:

Two pacemaker-like electronic devices were developed with the intention of electronically stimulating the baroreceptor, and tested in clinical trials. The first-generation

Rheos consists of surgically implanted electrodes leading to both carotids and a pacemaker unit implanted subcutaneously in the infraclavicular position. The second-generation system Baroreflex activation therapy (BAT) Neo uses a smaller, one-sided electrode with a significantly smaller aggregate. In clinical use only the second-generation system BAT Neo is currently available [36].

After the first 6 months of the therapy, 307 patients saw an average BP drop of 21 mmHg. These results have been accepted with caution as data are very limited. To the authors knowledge, there has been no assessment in differences in efficacy between sexes. Interestingly, in Europe, BAT have already received the CE Mark.

## 1.6 Thesis Aims

The aims of this thesis are threefold. First, verifying the earlier sexually-dimorphic observations in BRx control from the Schild lab. Second, to further explore acute dynamics by providing upwards of ten minutes of sustained stimulation. Third, compare the long term dynamics between continuous and burst paradigms within the sustained protocol. Low voltage (2V), low frequencies (2, 5 Hz) were chosen for several pragmatic reasons including depletion of neurotransmitters, resetting, and the potential for hypotensive, respiratory, or other crises involving chemosensory systems. The null hypothesis is that the sexual-dimorphic dynamics of the BRx in acute stimulation settings will not carry-over to the continuous and burst electrical stimulation paradigms of the sustained protocol.

## CHAPTER 2. MATERIALS AND METHODS

### 2.1 Introduction

All animal research protocols were approved by the Institutional Animal Care and Use Committee (IACUC) for the Purdue School of Science, Indiana University Purdue University Indianapolis (IUPUI). Adult rats (*Rattus*, Sprague-Dawley) were delivered to the small animal research center (SARC, vendor: Envigo) and generally allowed to acclimate to the vivarium for one or more days prior to study. A total of 24 rats, 14 males (Average Weight:  $331 \pm 37.9$  g; Average Age:  $75.1 \pm 7.2$  days) and 10 females (Average Weight:  $215 \pm 10.8$  g; Average Age:  $73.6 \pm 4.9$  days) were utilized for all approved experimental protocols.

Once transported to the lab, animals were anesthetized and prepared for surgery. A 3-lead ECG and femoral catheter were used to monitor HR and BP. Following a tracheotomy to facilitate natural breathing, the aortic depressor nerve was isolated through blunt dissection. The experimental paradigm consisted of a series of randomly selected stimulation paradigms to evoke a rapid and robust fall in arterial pressure, i.e. the depressor response of the baroreflex. Euthanasia and disposal were the last steps in the experimental protocol. Offline analysis of data was carried out at a later date.

The rat animal model was chosen for several reasons. The rat aortic BRx is a classic experimental preparation for evaluating reflexogenic function of myelinated and unmyelinated barosensory afferents [9]. The rat has a distinct, identifiable, purely mechanosensory afferent fiber termed the aortic depressor nerve (ADN). When acti-

vated electrically, a rapid and repeatable reduction in BP (the depressor response) occurs via the BRx [4].

## 2.2 Anesthetic

All experiments were performed with the animal resting at a surgical stage of anesthesia. Anesthetic was administered in two steps; an initial induction using a volatile anesthetic followed by intraperitoneal (IP) injection of a urethane and alpha chloralose cocktail.

The rat was placed in a transparent plastic airtight induction chamber for inhalation of 1mL of Isoflurane, USP (Henry Shein). Additional care was taken to maintain a physical barrier between the rat and the volatile anesthetic. Once movement ceased and respiration slowed the animal was removed from the induction chamber, weighted, and given an IP injection of a mixture of urethane (200 mg/mL) and alpha-chloralose (10 mg/mL) dosed at 0.8 mL per 100 g of body weight. The IP solution was prepared the day of the experiment and consisted of 20 mL of a 10 mg/mL refrigerated ( $\sim 4$  °C) stock solution of Urethane (Ethyle carbamate 97%, Agros Organics) and phosphate buffered saline (PBS) that was combined with 0.2 g of alpha-chloralose (chloralose, AT; Sigma Life Sciences). On account of the low solubility of -chloralose in PBS the mixture was gently heated (45 -50 °C) and stirred (300 rpm).

This two stage approach has proven to facilitate reliable and repeatable IP injection after which the animal was returned to the cage. After about 30 minutes the depth of anesthesia was assessed using a gentle pinch of the tail and footpad. Lack of responsive whisker movement, unlabored respiration and loss of motor response to skin stimulation collectively signaled that a surgical plane of anesthesia had been achieved.

## 2.3 Animal Preparation

With the rat maintaining a surgical plane of anesthesia, the ventral areas of the neck and left femur were shaved. The rat was placed on a steel rodent tray and secured with skin tape (Transpore, 3M). Care was taken to not restrict breathing. Body temperature was monitored using a rectal thermometer and maintained using an open-loop heating pad (HTP-1500 with ST-017 Soft-Temp Pad, Adroit Medical Systems). A standard 3-Lead ECG was used to monitor HR using hypodermic needles inserted subcutaneously about the left and right sides of the lower abdomen and the right leg. Alligator clips provided electrical continuity to a differential amplifier (Warner Instruments DP-311, Filter: Highpass: 0.1 Hz, Lowpass: 300 Hz, Gain: 1,000).

## 2.4 Surgical Preparation

The protocol consisted of three distinct surgical procedures, carried out in sequence: 1.) catheterization of the left femoral artery; 2.) tracheotomy; and 3.) blunt dissection and isolation of the left aortic depressor nerve (ADN).

### 2.4.1 Catheterization

Approximately 2-3 cm of the left femoral artery was exposed and freed from neighboring tissue. The artery was lassoed medially using suture to both block blood flow and secure the indwelling catheter. Lidocaine (Lidocaine 2%, Henry Schein) was dripped onto the exposed artery to relax smooth muscle and facilitate dilation. The lasso was pulled medially to clamp off the artery and a small cut was made in the vessel to insert the catheter. The catheter consisted of a short length ( 10 cm) of PE-100 tubing filled with heparinized saline (30 U/mL; Sagent Pharmaceuticals). Following tie down the catheter was attached to a T split (add name), 5 mL syringe

of heparinized saline, and the calibrated pressure transducer (Radnoti, CA) [Figure 2.1].

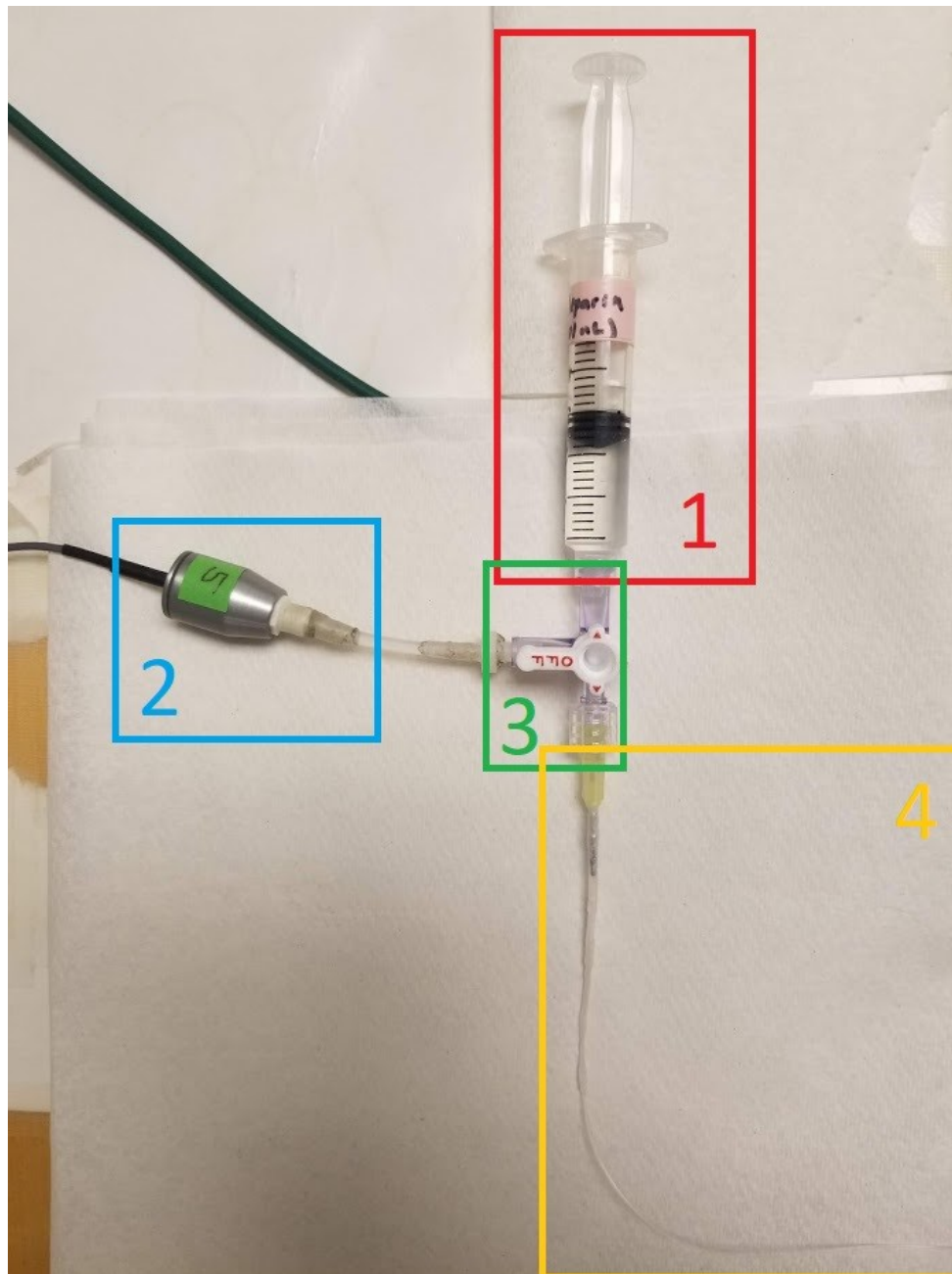


Fig. 2.1: Arrangement of components to monitor pressure in the femoral artery: 1) 5 mL syringe of heparinized (30 U/m) saline, 2) calibrated pressure transducer, 3) T-split luer lock, 4) PE-100 catheter.

### 2.4.2 Tracheotomy

A 2-3 cm midline incision about the ventral side of the neck provided access to the trachea and underlying musculature. A small length of trachea just below the larynx was separated circumferentially from neighboring vasculature and connective tissues. An incision was made between the tracheal cartilage rings and the tracheal tube was inserted [Figure 2.2]. The tracheal tube was an 5 cm length of Sublite tubing (Small Parts, Inc; Inner diameter: 1.75 mm). Should the animal exhibit labored or diminished respiration the tracheal tube was connected to a small animal respirator (Model 683 Small Animal Ventilator, Harvard Apparatus). Once a natural respiration rate was restored, the rat was removed from the respirator. All experiments carried out with the rat breathing spontaneously and at a natural rate and tidal volume.

### 2.4.3 Aortic Depressor Nerve Identification

Lateral to the trachea lies the left carotid artery and left cervical vagus [Figure 2.3]. The aortic depressor nerve (ADN) often travels near or within the sheath of the vagal nerve but as a separate and distinct collection of nerve fibers. Often, a small artery traveled along the length of the ADN that facilitated identification of the ADN trunk. The ADN was separated from the cervical vagus using blunted glass probes and placed orthogonally onto a Pt-Ir bipolar hook electrode (PBAA0875, FHC) that was secured to a micromanipulator (M3301R, World Precision Instruments). Verification that the nerve trunk was indeed the ADN was carried out using a short duration (10-20 sec) burst of 2V, 250 s pulses at a frequency of 50 Hz. Stimulation was maintained until a minimum in the depressor response had been achieved and arterial BP began to stabilize, often at a slightly more elevated pressure as a consequence of sympathetic activation. The particular stimulus amplitude, pulse width and frequency were utilized as these parameters have been shown to illicit a rapid and robust depressor response in both male and female rats. Concerns for nerve damage due to injecting a potentially unstable current density were mitigated with the afore-

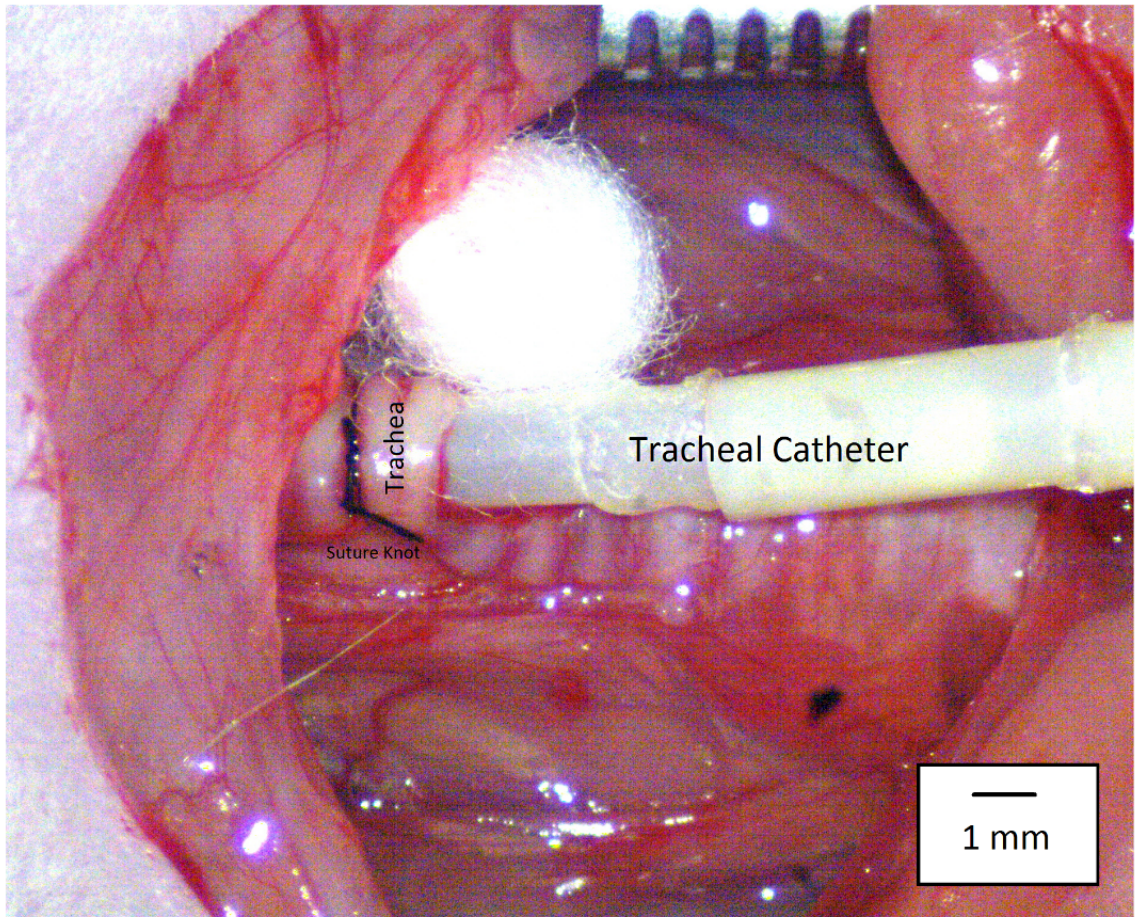


Fig. 2.2: Tracheostomy with tracheal catheter, trachea, and suture knot labeled.

mentioned pulse characteristic. Previous lab work demonstrated that 2V using this electrode configuration provided recruitment of all myelinated BR fibers in the ADN and none of the unmyelinated BR fibers with higher electrical thresholds [14].

Constant voltage was used instead of constant current for a few reasons. First, previous studies in the lab also utilized constant voltage and to corroborate previous results it would not make sense to change. Additionally, we are confident the charge will not cause any electrochemical damage as it is well within the water window for nerve tissue.

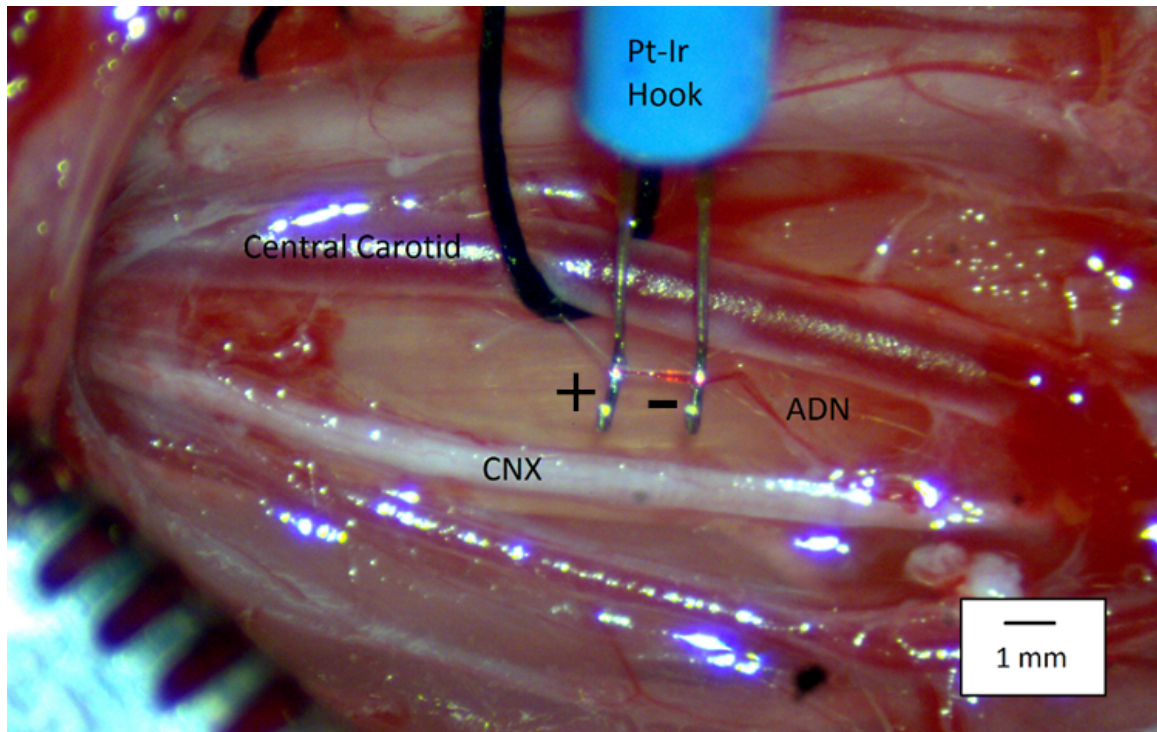


Fig. 2.3: Vagus Nerve (CNX), aortic depressor nerve (ADN), Platinum-Iridium hook, and central carotid artery.

## 2.5 Baroreflex Protocol

Following identification of ADN, the nerve trunk was completely transected using microsurgical vanna scissors, gently wrapped around the Pt-Ir hook with care taken so as not to stretch the delicate nerve fibers, and encapsulated in a mixture of Vaseline and mineral oil. BP and HR were monitored until a stable homeostatic autonomic plane was established marked by a  $MAP = 100 \pm 10$  mmHg and a HR between 4-6 Hz. A series of randomly selected stimulation paradigms were then carried out to assess the BRx depressor response. The ADN was never transected until a normal baseline had been established and following transection the stimulation protocols were never initiated until this normative baseline was reestablished.

There were two distinct protocols: acute and sustained. The sustained protocol consisted of continuous and burst paradigms. An effort was made to carry out all

paradigms in the same animal but often only a subset could be completed before the animal failed to return to baseline pressures following ADN stimulation. Each pulse train was generated using a Master 8 Stimulator (A.M.P.I., Israel) with a pulse width (PW) of 250 s. This fed into an electrical stimulator set at a regulated 2V amplitude (ISO-Flex Stimulus Isolator, A.M.P.I.).

### 2.5.1 Stimulation Paradigms

Three stimulation paradigms were carried out to assess BRx control of HR and BP: acute, continuous, and burst. Acute stimulation paradigms were carried out to verify the experiment was producing results consistent with earlier studies where 2V of stimulation was sufficient to recruit all myelinated BR fibers in the ADN. Continuous stimulation paradigms were carried out to assess the steady state depressor response and subsequent recovery of myelinated BR afferents. Of most interest is how the BRx would respond to an extended, continuous stimulation of the ADN. Like the continuous paradigms, burst paradigms focused on patterned pulse train and their effect on the steady state BRx response of BP and HR. Unlike the continuous paradigm, each fundamental pulse had 3 subsequent pulses with inter beat spacing of 20 s [Figure 2.4]. This was carried out to better mimic the evoked BR discharge that arises from pulsatile arterial pressure.

The acute stimulus paradigms were similar to those report in Cruz-Chavez et al [9] with stimulation frequencies of 1, 2, 5, 10, 20, and 50 Hz. However, unlike these previous studies the duration of stimulation for these acute paradigms was not fixed but only maintained until there was clear indication of a minimum in the depressor response ( 10-20 seconds). Previous reports suggest electrical activation at low stimulation intensities ( $< 3$  V) activate only A type BRs. In contrast, high stimulation intensities (18-20 V) maximally activated A- and C- type BRs [4]. Other studies expanded upon this work by focusing on recruitment at differing frequencies:

finding maximal depressor responses at higher frequencies [9]. The depressor response to trains of stimulation were digitally recorded.

The continuous paradigms consisted of continuous-trains of 250 s pulses at fixed frequencies of either 2 or 5 Hz and at a fixed stimulation magnitude of 2V and for a duration of 600 seconds. Such low stimulation frequencies were utilized because these are at or just below the normal resting heart rate for the rat which generally leads to discharge of myelinated BR fibers that align with the systolic pulse in BP. A duration of 600 seconds was selected as a compromise between generating an adequate length of ECG data for subsequent heart rate variability (HRV) analysis and lessening the potential for neurotransmitter depletion at the first synapse in the NTS on account of the synchronous recruitment of all myelinated BR fibers in the ADN [4] .

Burst paradigms, like continuous, consisted of continuous trains of 250 s pulses at fixed frequencies of either 2 or 5 Hz at a fixed stimulation magnitude of 2V for a duration of 600 seconds. Unlike continuous paradigms, each pulse was followed by 3 successive pulses with 20 s spacing [Figure 2.4]. This allowed for an equivalent number of pulses as would be generated in a continuous 8 and 20 Hz response, respectively. These continuous 8 and 20 Hz equivalents were chosen since these frequencies showed the largest amount of difference in the peak depressor response of previous lab work [3].

## 2.6 Data Acquisition and Recording

Three-channel acquisition of amplified ECG, BP, and pulse train generator output were continuously sampled at 10 kHz using a NI DAQ USB-6212 (National Instruments; Input Voltage Range: +/- 10V) and Mr. Kick III acquisition software (Aalborg, Denmark). Analog input channels to the USB-6212 were as follows: 0: DP-311 output (ECG), 1: Voltage transducer output (BP), 2: Master-8 output (ISO-Flex stimulator input). Master-8 output were pulses of fixed duration frequency which aided as a toggle line for start/stop referencing.

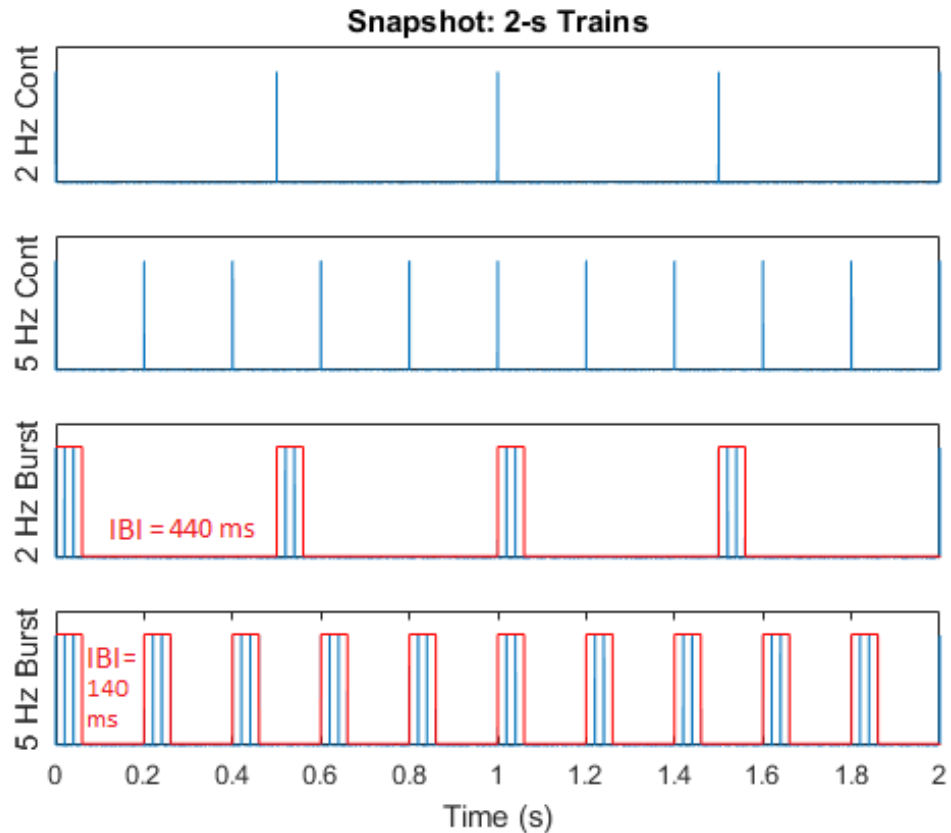


Fig. 2.4: A 2-s snapshot illustrating the difference between continuous and burst pulse trains, IBI = inter-burst interval in milliseconds (ms).

## 2.7 Euthanasia

Upon completion of the experimental protocol, the animal was euthanized with a lethal dosage of 3-molar KCl to the heart via a 5 mL syringe and 21G needle. A bilateral pneumothorax was also carried out as a physical means of ensuring euthanasia. Should problems arise within the experiment such as an obvious autonomic crisis e.g. unstable BP or HR, or respiration suggesting a loss of homeostasis, or surgical failure e.g. both femoral arteries failed to be catheterized or inability to find the left ADN, the animal was euthanized in a similar manner.

## 2.8 Data Analysis

Data analysis was performed using custom scripts written for MATLAB 2017b (Mathworks, Nitick, MA). Data were first visually inspected to ensure no adverse events or bias occurred during the recording and then digitally filtered. Adverse events include but are not limited to electrical contamination of the signal, arbitrary perturbations of physiological conditions e.g. gasps, apneustic breaths, twitching, or diaphragm spasms. Perturbations of physiological conditions include unexplained swings in BP or HR. As the Master-8 provided a reference point for stimulation timing, a custom script facilitated automatic identification of the minimum depressor response.

All acute BP runs were digitally filtered at 100 Hz using a 3rd order low pass butterworth filter (Matlab butter function). This was applied to eliminate high frequency noise originating from the encoding of pressure to voltage by the Radnoti pressure transducer.

Sustained, burst, and in-tact BP recordings were first digitally filtered at 100 Hz using a 3rd order low pass butterworth filter (for high frequency noise) and then further filtered with a 3rd order low pass butterworth filter with a 1 Hz cutoff (Matlab butter function). The second filter was used to provide a clearer picture of the oscillatory nature of the signal over duration of the run by minimizing high frequency systolic/diastolic oscillations.

Acute data (BP and HR) were segmented into two epochs [Figure 2.5]:

- 1.) BASELINE A (-10 - 0 sec): a 10-s baseline period taken just prior to nerve stimulation and
- 2.) BASELINE B: a 1-s epoch about the absolute minimum of the depressor response ( $\pm$  500 millisecond) during stimulation.

Sustained datasets were segmented into three epochs (times listed relative to stimulation onset) [Figure 2.7]:

- 1.) BASELINE X (@ -30 0 sec): a 30-s baseline period taken just prior to nerve stimulation;
- 2.) BASELINE Y (@ 570-600 sec): a 30-s period taken just prior to the end of sustained stimulation;
- 3.) BASELINE Z (@630-660 sec): a 30-s period taken 30 seconds after the end of stimulation.

In addition, BASELINE A and BASELINE B values were recorded for sustained datasets for comparison to acute responses. Figures 2.5 and 2.6 illustrate segmentation for a typical acute depressor response while Figure 2.7 illustrates segmentation for a typical sustained depressor response.

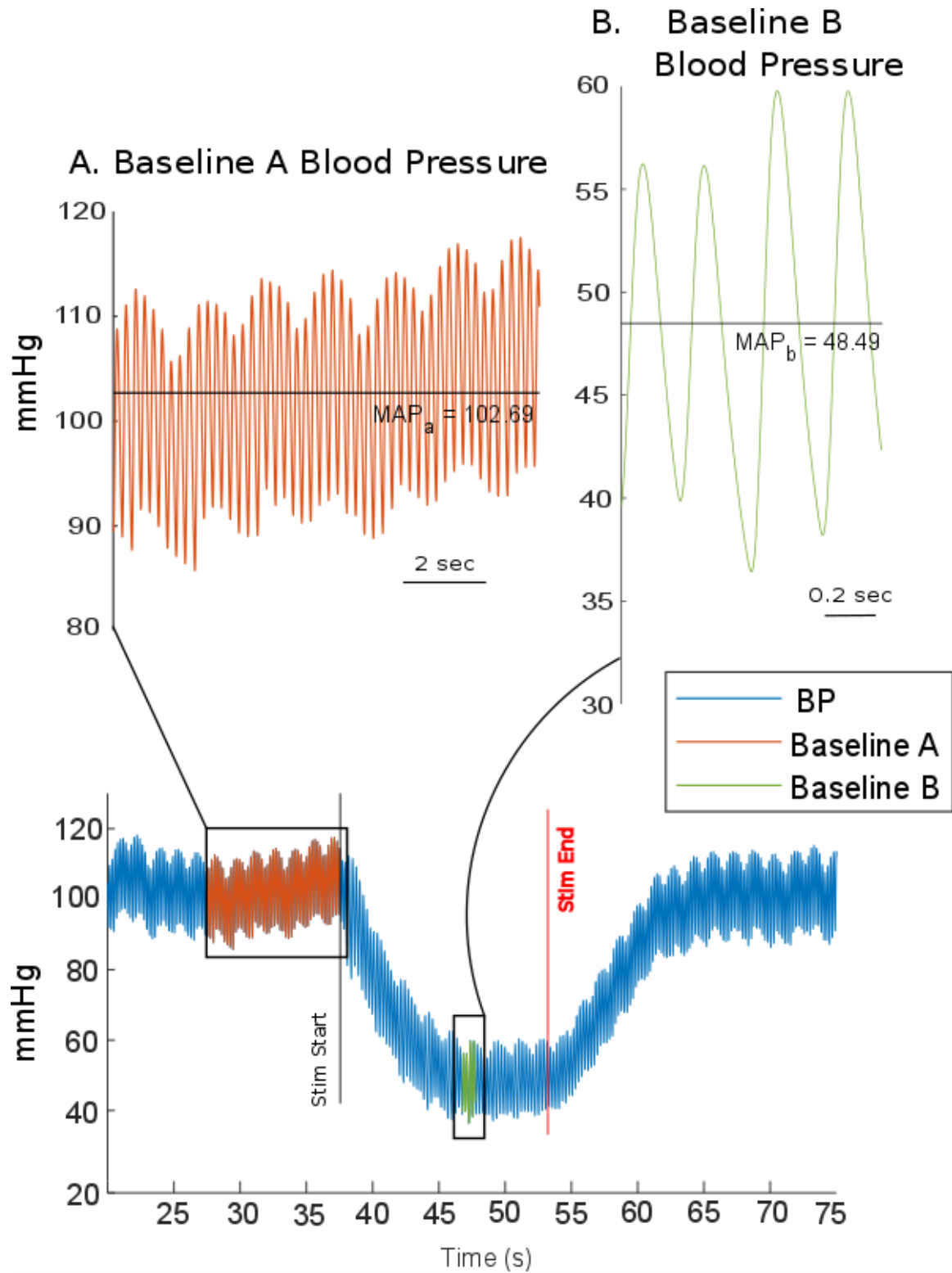


Fig. 2.5: Typical depressor response (bottom) with segmented baseline A (A - orange) and baseline B (B - green). Average for baseline A and B were 102.69 and 48.49 mmHg, respectively.

### Typical 50 Hz Depressor Response (F: B81119)

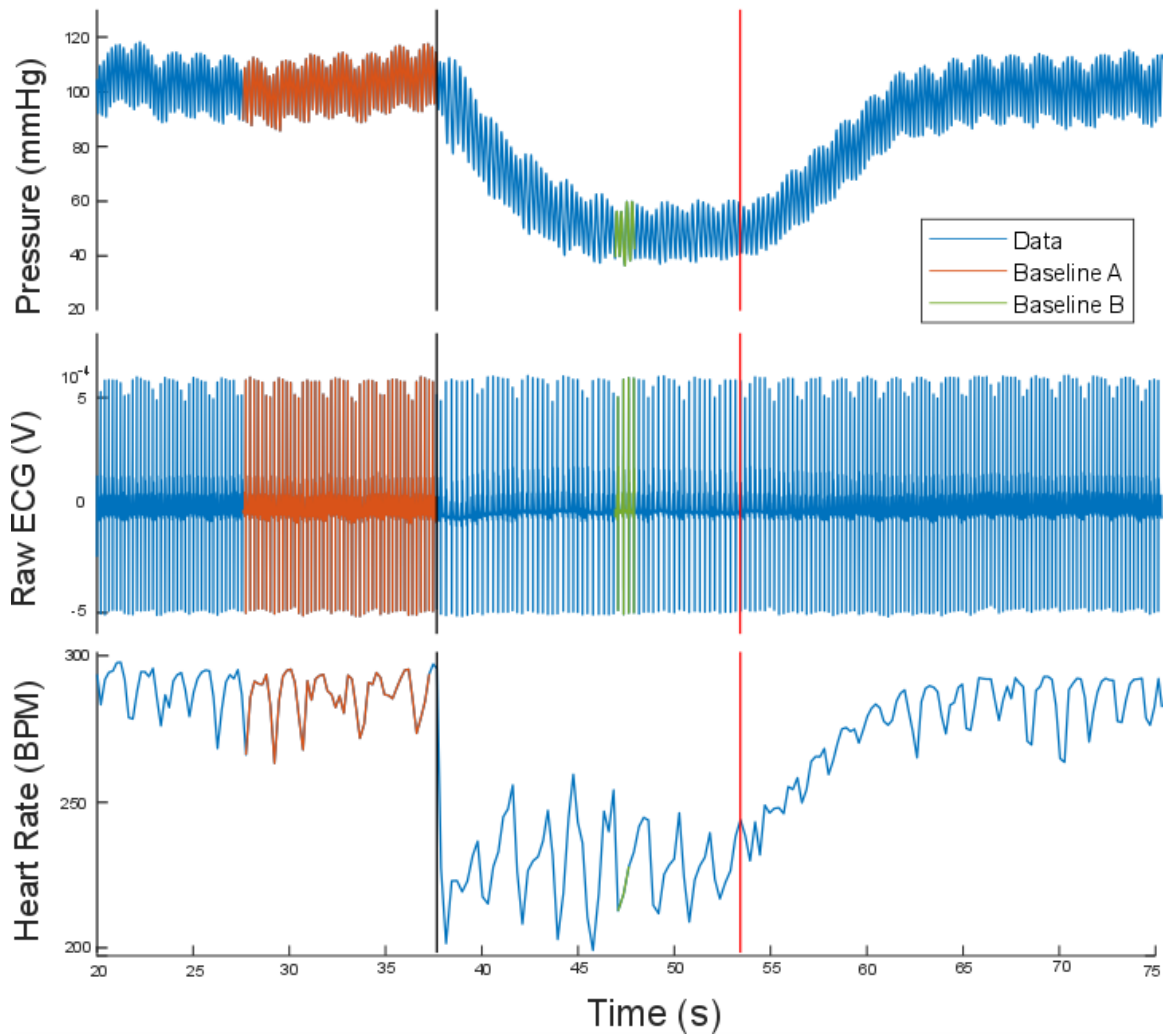


Fig. 2.6: Typical 2V 50 Hz acute depressor response with associated blood pressure (top), raw ECG (middle), and converted heart rate in beats per minute (bottom). Rapid reduction in pressure and heart rate was seen following stimulation (vertical black line) of ADN until stimulation end (red vertical line) allowed recovery.

BASELINE A (orange) 10 seconds of pressure prior to stimulation onset.

BASELINE B (green) 1 second of pressure about the peak depressor response.

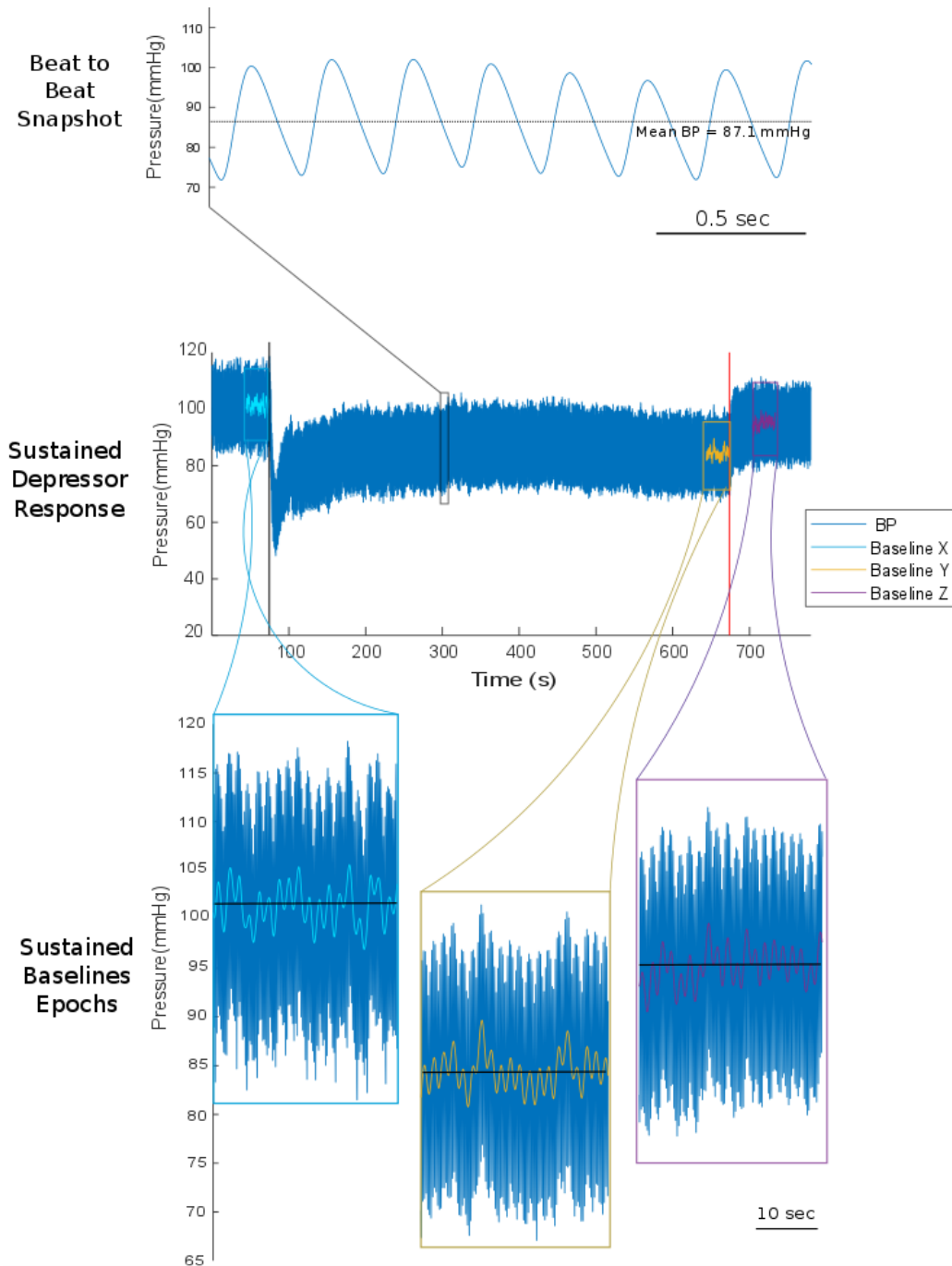


Fig. 2.7: Typical 2V 5 Hz sustained depressor response (middle). Small 2-s epoch of beat to beat blood pressure (top). A rapid reduction in pressure was seen following stimulation (black vertical line) of ADN until stimulation end (red vertical line) allowed recovery. Associated epochs (bottom) were segmented and plotted. BASELINE X (cyan) 30 seconds of pressure prior to stimulation onset. BASELINE Y (gold) 30 second of pressure taken just prior to end of stimulation. BASELINE Z (magenta) 30 seconds of pressure taken 30 seconds after the end of stimulation.

### 2.8.1 Calculations

#### Acute

Depression response of the BRx was quantified as a percent change from baseline i.e. the ratio of the moving-average of BASELINE B and moving-average of BASELINE A multiplied by 100. Termed delta of mean arterial pressure or dMAP [Eq 2.1], this percentage quantifies the normalized peak change in mean arterial pressure relative to resting arterial pressure:

$$\%dMAP_{AVC} = 100 * \frac{Average(BaselineA) - Average(BaselineB)}{Average(BaselineB)} \quad (2.1)$$

Heart rate was converted to beats per minute (BPM) by calculated the R peak to R peak time interval in the ECG and converting to a frequency (Hz). The frequency was then multiplied by 60 to quantify BPM. The time to the peak fall in blood pressure (TTP) was also calculated by finding the time difference between stimulation onset and the minimum point used to calculate BASELINE A.

#### Sustained

The dMAP was also useful for finding the change in mean arterial pressure relative to the resting arterial pressure between BASELINEs X and Y (X v Y, Eq 2.2) as well as between BASELINEs X and Z (X v Z, Eq 2.3). X v Y quantifies the difference between BASELINE X and BASELINE Y, while X v Z quantifies the difference BASELINE X and BASELINE Z.

$$\%dMAP_{XvY} = 100 * \frac{Average(BaselineX) - Average(BaselineY)}{Average(BaselineX)} \quad (2.2)$$

$$\%dMAP_{XvZ} = 100 * \frac{Average(BaselineX) - Average(BaselineZ)}{Average(BaselineX)} \quad (2.3)$$

In addition to these new % dMAP calculations, TTP and BPM were calculated as they were in BASELINE A and BASELINE B but using BASELINE X, Y, and Z.

## 2.9 Timeline of Experiment

Duration of experiment typically lasted 3 to 8 hours and was mostly dependent upon establishing a stable autonomic plane [Table 2.1]. Anesthetic administration lasted approximately 45 minutes to an hour, given that the IP injection did not go into any alternative tissues. Animal preparation took 10 minutes.

An ideal surgical preparation lasted approximately 20 minutes for the femoral catheterization, another 10 for the tracheotomy, and 20 minutes for identification of the ADN. A non ideal preparation lasted upwards of 40 minutes for the femoral catheterization, 25 minutes for the tracheotomy, and upwards of 90 minutes for identification of the ADN. In total, an ideal surgical prep lasted 50 minutes while a non ideal surgical prep lasted 155 minutes.

Substantial time existed between identification of the ADN and the animal reaching a stable autonomic plane. Ideally, this period lasted 15 minutes. On a day where anesthetic depth was hard to assess or the animal was hypertensive/hypotensive, waiting could persist for up to 120 minutes.

After identification of ADN and verifying a robust and typical BRx response, acute paradigms were carried out. If an In-Tact paradigm was attempted, acute paradigms would follow. Each acute paradigm took no more than 15 seconds to carry out, but a 3-5 minute latency separated subsequent stimulation to allow the animal to return to baseline. With 6 frequencies in the acute paradigms, total time varied from 18 to 30 minutes. Once completed, sustained, burst, and high-voltage acute paradigms were randomly selected. 10 minutes were required of each recording (time before/after to assess homeostatic balance), trials averaged 15 minutes with a minimum of 5 minutes latency separation. For a full two trials of 2 and 5 Hz frequencies in sustained, burst, and in-tact sets, total time reached around 100 minutes. Some animals were unable

to run the full extent of sustained, burst, and in-tact, so 2 of one would be considered a successful preparation (40 minutes).

Following the experimental endpoint, the animal was euthanized and the surgical area cleaned and disinfected. The process of cleaning the tools, table, and disposing of the rat took 15 minutes.

In addition, anesthetic preparation of urethane and alpha chloralose was done each day a preparation was to be carried out. Due to the low solubility of alpha chloralose in PBS, the mixture had to be heated (50 C) and stirred (300 RPM) for a minimum of 60 minutes and as long as 180 minutes.

Table 2.1: Typical Timeline for Experimental Preparation.

Preparation Step	Description	Time Required (minutes)
		Range
Anesthetic Preparation	Dissociation of Alpha Chloralose in Urethane	180 - 60
Anesthetic Administration	Induction, IP injection	45 - 60
Animal Preparation	Shave, ECG setup	10 - 10
Surgical Preparation	Femoral catheterization, tracheostomy, identification of ADN	50 - 155
Stable Autonomic Plane	BP: 100 mmHg +/- 10 mmHG; HR: 4-6 Hz	15 - 120
BRx Protocol	Acute Paradigms	18 - 30
	Sustained Paradigms	40 - 100
Wrap Up	Euthenasia, Clean up	15
Total (minutes)		373 - 550
Total (hours)		6.22 - 9.17

## CHAPTER 3. RESULTS

### 3.1 Introduction

The main objective of this work is to investigate BRx neural control on heart rate and blood pressure through selective activation of BR fibers. The null hypothesis is that the sexually dimorphic depressor response observed in acute stimulation will not carry over to the sustained paradigms. Distinct and duration-varying experimental protocols were used to quantify the reflexogenic and steady-state differences associated with selective activation of the arterial baroreflex through electrical stimulation of the left ADN in male and female rats. Specifically, this includes (1) verifying the repeatability of parasympathetic mediated reductions of mean arterial pressure in male and female rats through acute stimulation of myelinated fibers. Further, the author will (2) extend the duration of stimulation to establish a functional understanding of steady state responses to BRx neural control of HR and BP. And finally, (3) a comparison of sustained continuous versus sustained bursts of applied electrical stimulation will be assessed.

Recruitment threshold(s) for myelinated BR fibers are well below that of unmyelinated BR fibers [9]. Consistent with previous studies in Schild lab, selective recruitment of myelinated fibers is possible through a standard 2V pulse magnitude as this guarantees recruitment of all low-threshold myelinated fibers and none of the high-threshold unmyelinated fibers. Reflexogenic studies involved 14 males (Average Weight:  $331 \pm 37.9$  g; Average Age:  $75.1 \pm 7.2$  days) and 10 females (Average Weight:  $215 \pm 10.8$  g; Average Age:  $73.6 \pm 4.9$  days) rats.

## 3.2 Research Aims

Aim 1: To reassess previous observations of a sexual dimorphic parasympathetic mediated reductions in MAP and HR through selective activation of BR afferents

Aim 2: To extend the understanding of the steady-state neural responses of the autonomic nervous system in maintaining MAP and HR through sustained activation of the baroreflex response

### 3.3 Aim 1: Verifying Acute Baroreflex Dynamics

To corroborate the evidence of sexual dimorphism in the reflex response, an in situ BRx study was prepared. Selective electrical recruitment of all low threshold, myelinated BR fibers and no high threshold, unmyelinated BR fibers was possible through stimulation intensity selection of 2V. Blood pressure and heart rate was continuously monitored via a femoral catheter and 3 lead ECG in urethane and alpha-chloralose anesthetized male and female rats.

Following surgical isolation and identification of the ADN, the nerve was placed on a Pt-Ir bipolar hook electrode. To verify its identity, the nerve was electrically activated using a brief ( 5 second) 50 Hz burst of 2V, 250-microsecond pulses. A rapid and robust depressor response verified the nerve on the hook was the left ADN. Following confirmation, the nerve was cut caudally removing any spontaneous afferent BR discharge. The nerve was gently wrapped around the cathode hook, taking care to maintain contact with the anode, and covered in a mixture of mineral oil and Vaseline.

BP and HR were monitored until a stable homeostatic autonomic plane was established marked by a  $MAP = 100 \pm 10$  mmHg and a HR between 4-6 Hz. Stimulation pulses of 250 microseconds were applied at randomly selected frequencies of 1, 2, 5, 10, 20, and 50 Hz.

Stimulation was maintained until there was clear indication of a minimum in the depressor response ( 10-20 seconds) [Figure 2.5]. This minimum in the depressor

response was initially verified qualitatively, and further analyzed quantitatively offline. Two epochs were established for comparing resting homeostatic values to those during stimulation: baseline A and baseline B. Baseline A consisted of a 10 second window just prior to the stimulation onset. Conversely, baseline B was a 1 second window about the minimum peak fall in BP [Figure 2.5].

### 3.3.1 Blood Pressure Changes

Inconsistent with previous observations, the average resting MAP in male rats was similar to that of female rats,  $99.47 \pm 8.89$  mmHg and  $100.02 \pm 6.69$  mmHg, respectively. To better quantify the depressor response during acute stimulation, a percent change in the mean arterial pressure (% dMAP) was calculated [Figure 3.2]. By finding the difference between the average BP of baseline A and average of baseline B, as well as dividing by the average of baseline B, a normalized dMAP can be calculated for each frequency and compared between populations.

In female rats, a depressor response and decrease in heart rate could be reliably evoked at lower stimulation frequencies than in age-matched males [Figure 3.1].

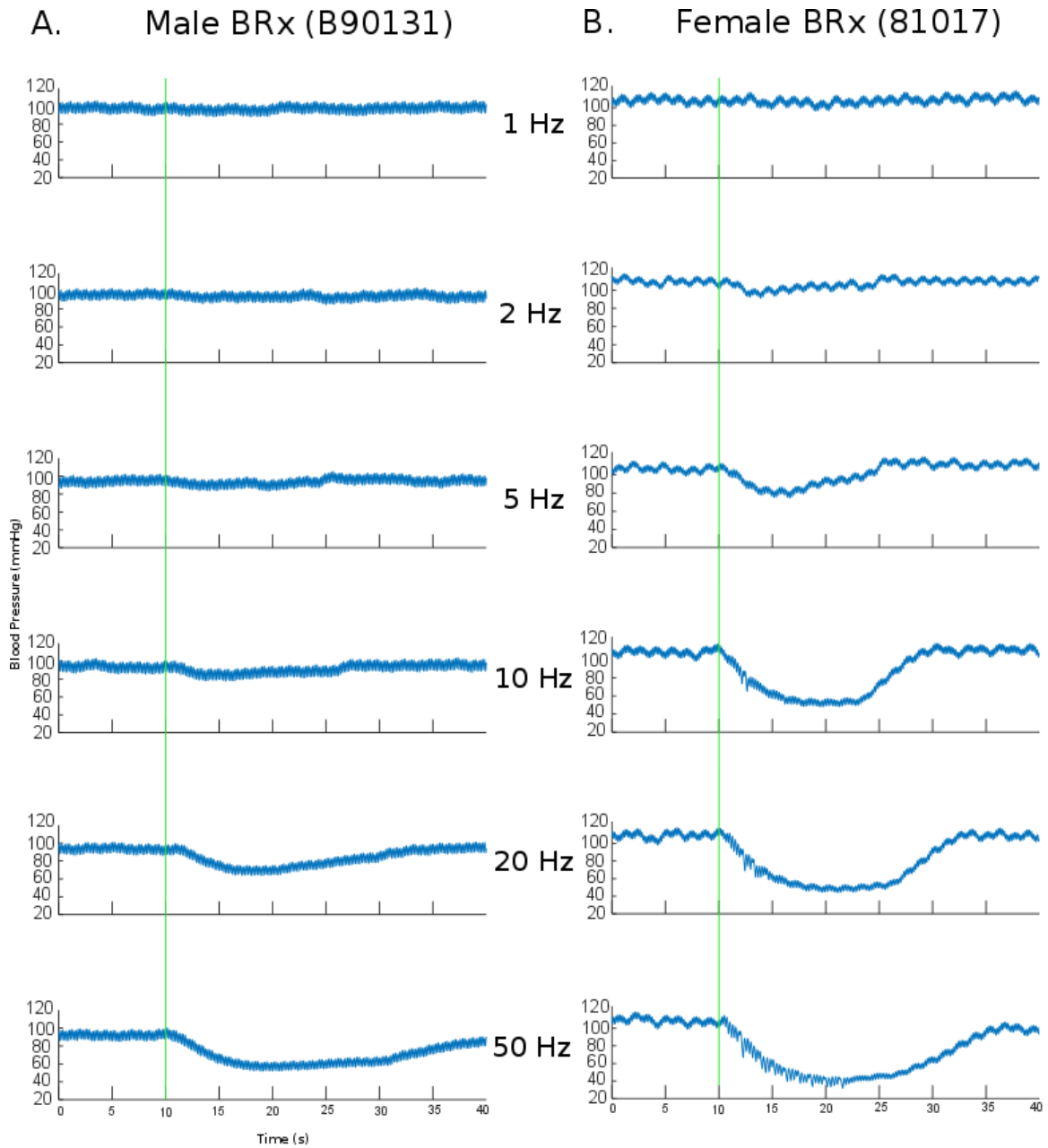


Fig. 3.1: Low threshold myelinated afferents in female rats elicit the BRx at lower stimulation frequencies than in male rats. In situ, bipolar stimulation of the left ADN at standard 2V. Stimulation onset elicited a rapid fall in BP albeit with differences across the response from male (A) and female (B) rats. Each trial consisted of a non-fixed duration of stimulation at randomly selected frequencies maintained only until there was a clear indication of a minimum in the depressor response. Runs are arranged here in ascending order, with a green dashed line indicating stimulation start at  $t = 10$  seconds.

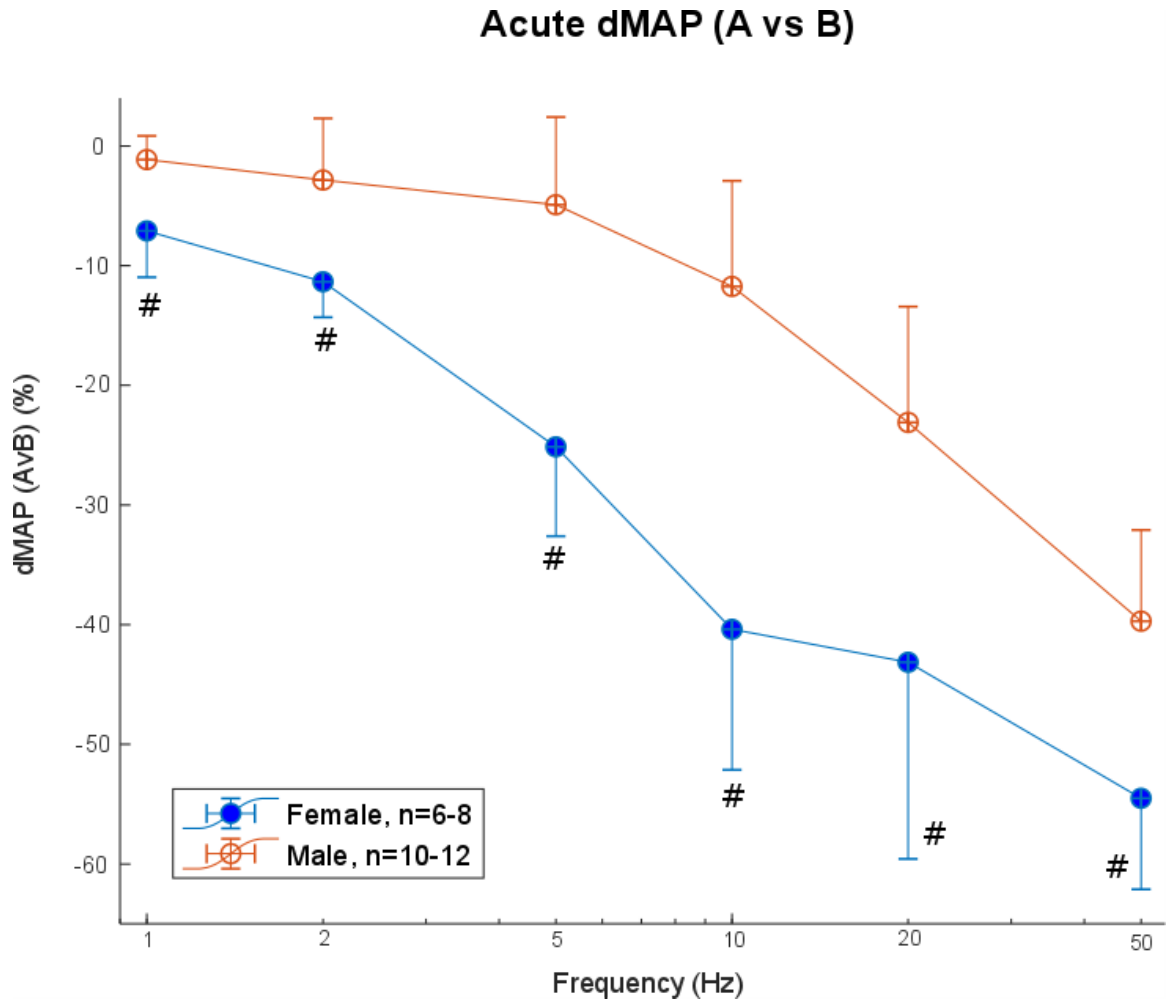


Fig. 3.2: The BRx in female rats elicits a greater depressor response at low rates of 2V bipolar stimulation of the left ADN than in male rats. Average % changes in MAP evoked through bipolar stimulation of the left ADN using randomly selected frequencies (1 to 50 Hz) at a regulated 2V amplitude. Data are means  $\pm$  SD, #  $p < 0.01$ .

### 3.3.2 Heart Rate Changes

The depressor response is often accompanied by a decrease in the R-peak to R-peak interval (RRI). RRI can be used to estimate beats per minute (BPM) by converting the time between peaks into a frequency and multiplying by 60 [Figure 2.5].

Resting BPM is lower in females than males,  $296.2 \pm 43.0$  BPM and  $322.17 \pm 32.0$  BPM, respectively. HR variability is an unavoidable consequence of this protocol since BP is a continuous measure and HR depends upon the pulsatile nature of the heart. Because of this, estimating the heart rate for the short 1 second epoch about the peak depressor response (baseline B) can be difficult. Females can have as little as three r-peaks during a strong depressor response where RRI can change upwards of 40%. Nonetheless, a reliable trend can be quantified by estimating the percent change in the BPM. To better quantify the change in BPM during acute stimulation, an average in BPM about the minimum depressor response was calculated [Figure 3.3].

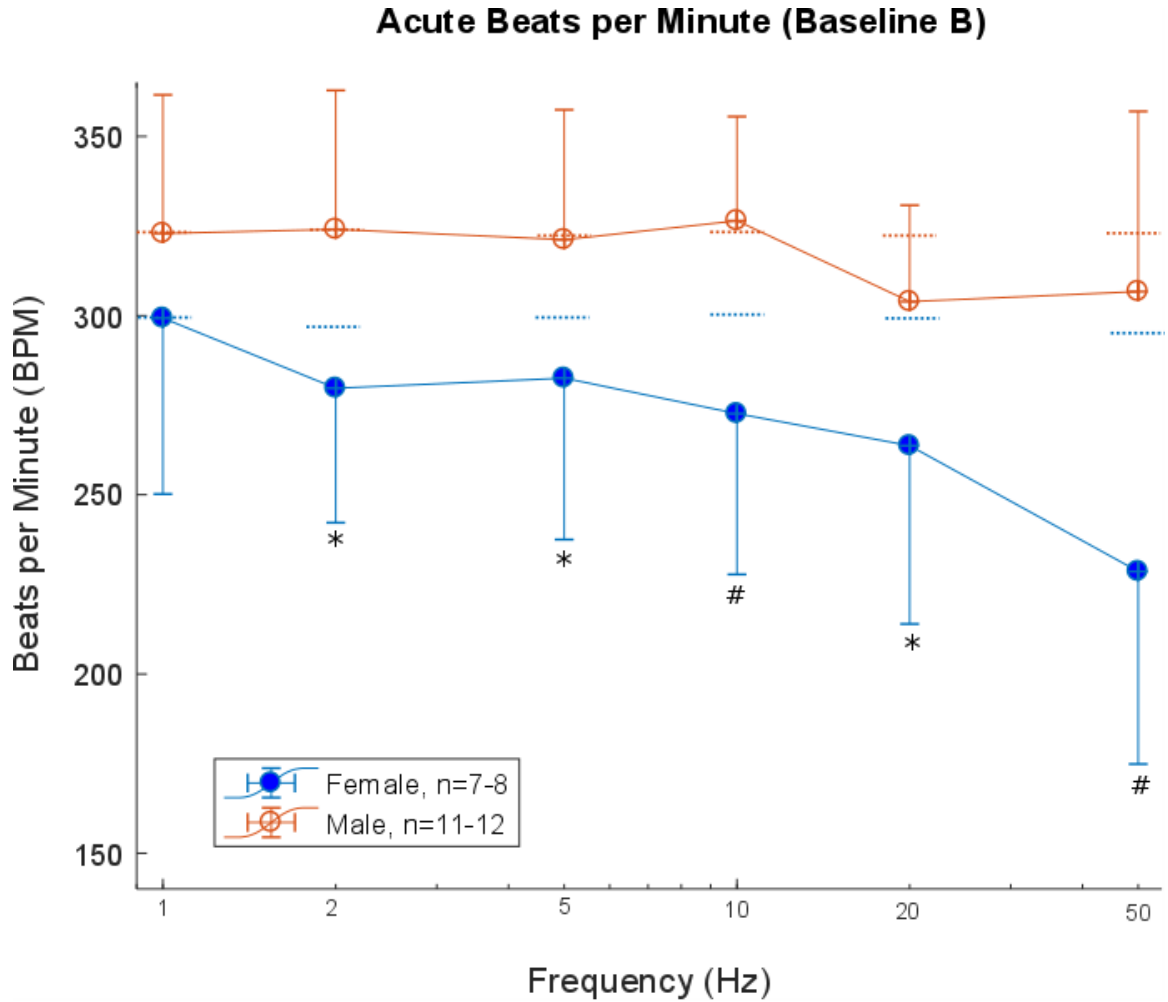


Fig. 3.3: The BRx in female rats elicits a greater change in heart rate at rates of 2V bipolar stimulation of the left ADN than in male rates. Average changes in the Baseline B HR evoked through bipolar stimulation of the left ADN using randomly selected frequencies (1 to 50 Hz) at a regulated 2V amplitude. Dotted lines denote the average resting HR prior to stimulation onset. Data are means  $\pm$  SD, \*  $p < 0.05$  and #  $p < 0.01$ .

### 3.3.3 Timing Characteristics

In addition to changes in BP and HR, certain timing characteristics of the reflex response were taken into consideration. The time to peak fall in BP, or TTP, denotes the time required for BP to fall from the resting mean (prior to stimulation) to the peak depressor response [Figure 3.4]. It is important to note the limitations of this measure as it can be heavily influenced upon factors related to catheter components (see discussion). Tip sharpness, age of animal, and intermittent blockages are just a few of the factors that can introduce variability into this measure. These data help contribute to the derivative encoding mechanisms intrinsic to mechanotransduction by the BRs.

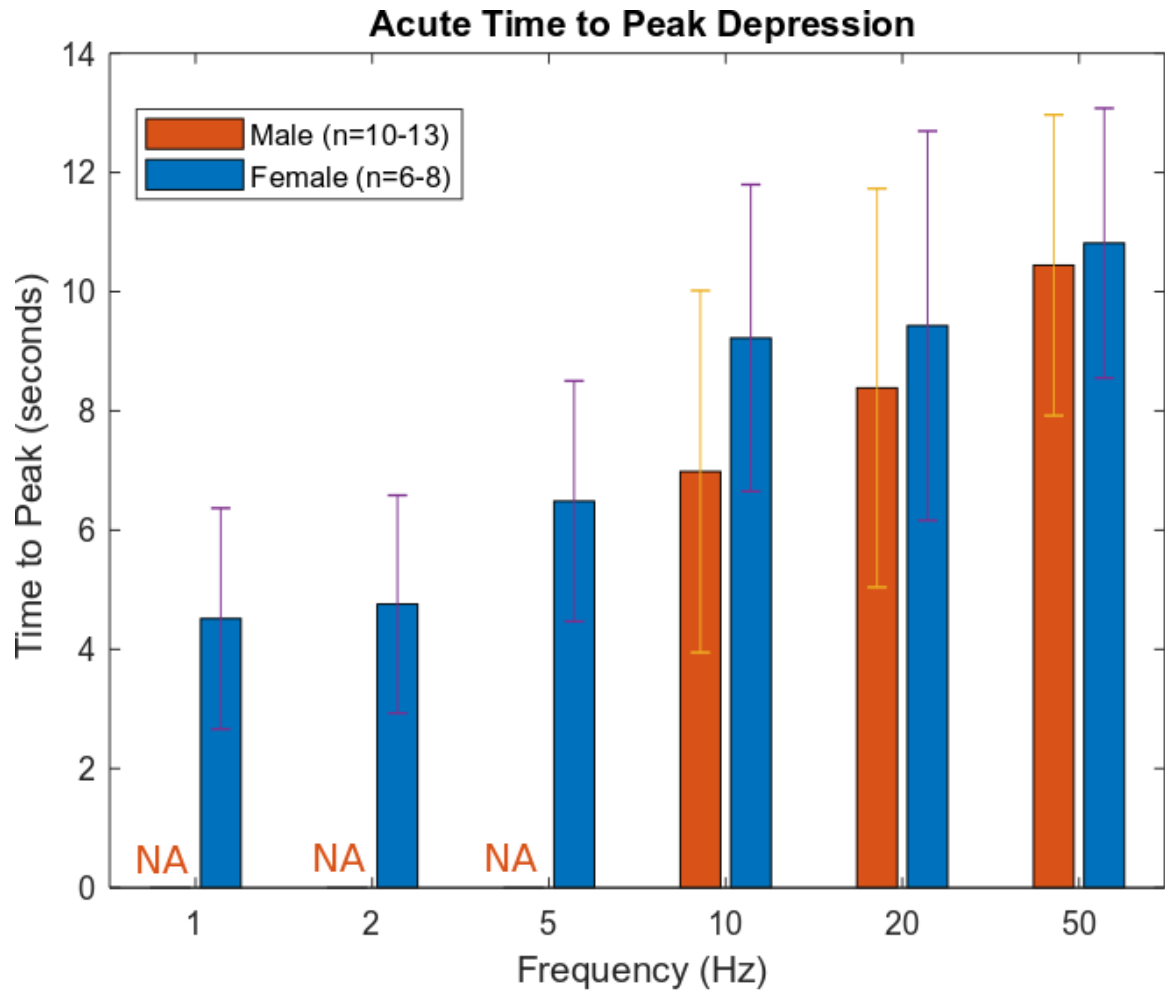


Fig. 3.4: Acute time to peak fall in blood pressure response following the onset of acute stimulation differs between male and female rats. Average time to peak (TTP) in seconds for randomly selected stimulation frequencies (1-50 Hz). Data are not present for male response in frequencies 1, 2, and 5 Hz due to there being no depressor response present. Data are means  $\pm$  SD.

### 3.4 Aim 2: Sustained Baroreflex Dynamics

Much like acute electrical stimulation, the depressor response persists as the duration of stimulation is extended. The author carried out a sustained (10-minute) stimulation of the left ADN to assess the steady state response of the BRx and to observe if the sexually dimorphic aspects of parasympathetic mediated BP and HR decreases persisted with the extended duration. Like that of Aim 1, a regulated 2 V pulse amplitude was chosen since this magnitude had been shown to reliably recruit many of the myelinated BR fibers and was far below the magnitudes needed to activate unmyelinated BR fibers.

Stimulation pulses of 250 microseconds were applied at randomly selected frequencies of 2 and 5 Hz. One sustained paradigm followed a fixed or continuous stimulation train (continuous), while the other included a burst of pulses (burst) [Figure 2.4]. The burst paradigm was selected to better mimic the naturalistic and pulsatile generation of APs in BR afferents. Burst paradigms, like continuous, consisted of trains of 250 s pulses at fixed frequencies of either 2 or 5 Hz at a fixed stimulation magnitude of 2V for a duration of 600 seconds. Unlike sustained paradigms, each pulse was followed by 3 successive pulses with 20 s spacing [Figure 2.4]. This allowed for an equivalent number of pulses as would be generated in a continuous 8 and 20 Hz response, respectively. These 8 and 20 Hz equivalents were chosen since these frequencies showed the largest amount of variability in the acute paradigm [Figure 3.2]. Segmentation into baseline X, Y, and Z was completed just as in continuous paradigm. Offline analysis included the measures carried out in Aim 1, i.e. peak depressor responses, as well as a detailed look at the steady state responses following 600 seconds of stimulation.

### 3.4.1 Comparison of Peak Depressor Response Dynamics

The relative differences in the short-term BP and HR changes in sustained stimulation paradigms were compared to acute paradigms. To first understand the short-term differences in the depressor response, % dMAP was calculated at 2 Hz [Figure 3.5] and 5 Hz [Figure 3.6] for continuous and burst paradigms. Subsequent changes in beats per minute are listed below.

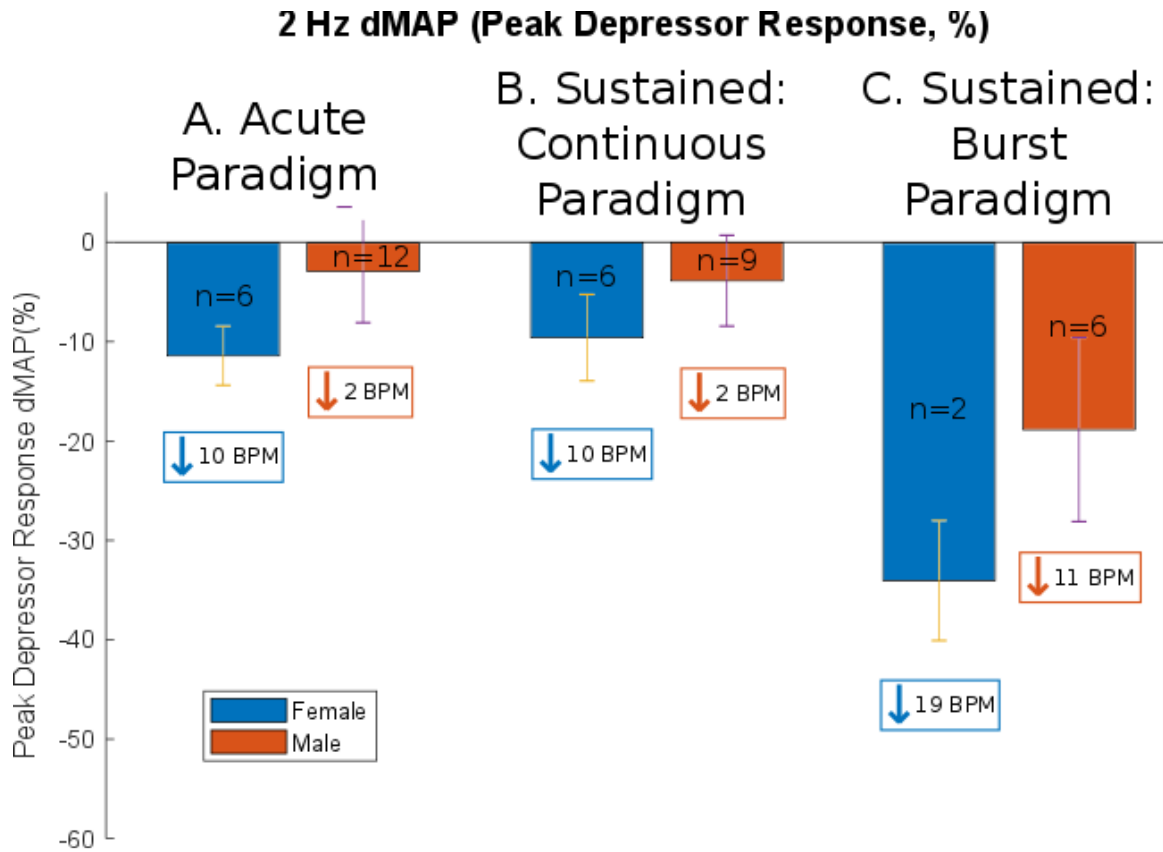


Fig. 3.5: Percent change in mean arterial pressure between baseline A and baseline

B following the onset of 2 Hz stimulation differs between male and female rats.

Average percent change in blood pressure (dMAP) for acute (A), continuous (B),

and burst (C) paradigms. Data are means  $\pm$  SD.

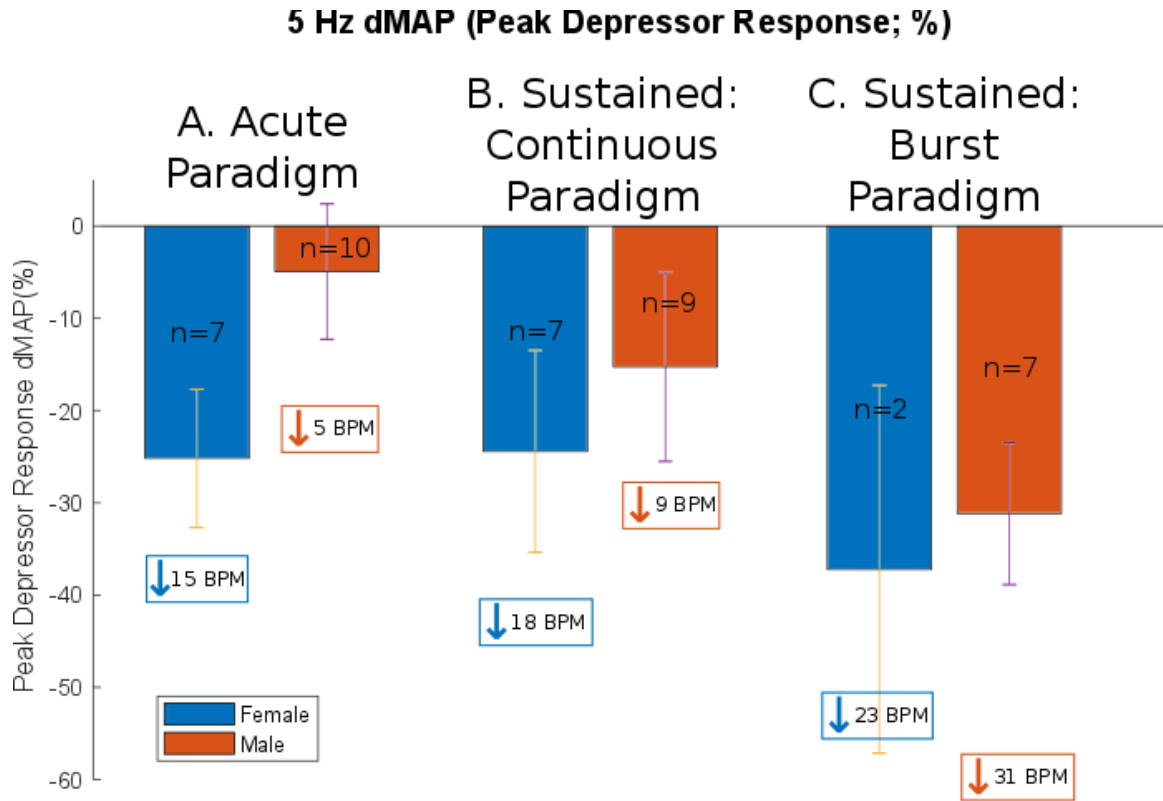


Fig. 3.6: Percent change in mean arterial pressure between baseline A and baseline B following the onset of 5 Hz stimulation differs between male and female rats. Average percent change in blood pressure (dMAP) for acute (A), continuous (B), and burst (C) paradigms. Data are means  $\pm$  SD.

To better understand the time associated with the magnitude decreases in BP, a time-sensitive calculation was employed. Time to peak fall in BP was calculated for the 2 Hz [Figure 3.7] and 5 Hz [Figure 3.8] short-term depressor responses between males and females.

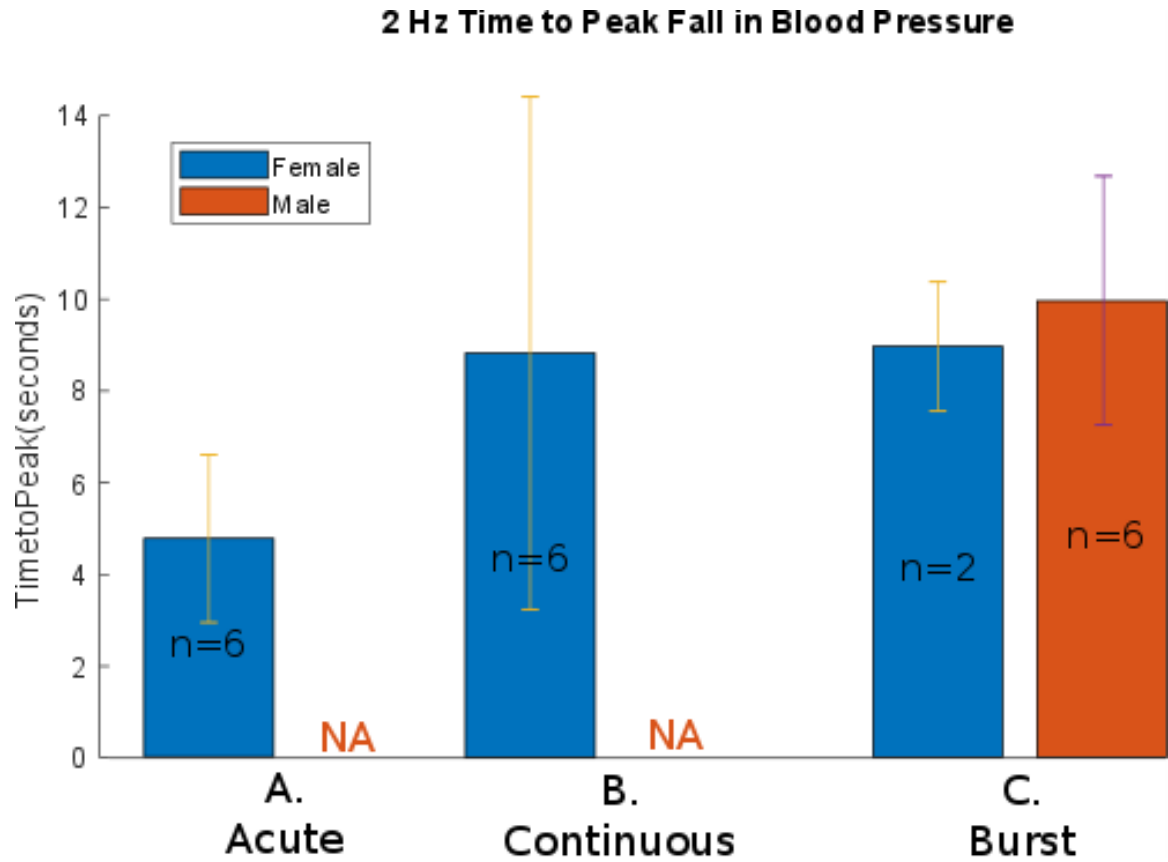


Fig. 3.7: Percent change in mean arterial pressure between baseline A and baseline B following the onset of 5 Hz stimulation differs between male and female rats. Average percent change in blood pressure (dMAP) for acute (A), continuous (B), and burst (C) paradigms. Data are means  $\pm$  SD.

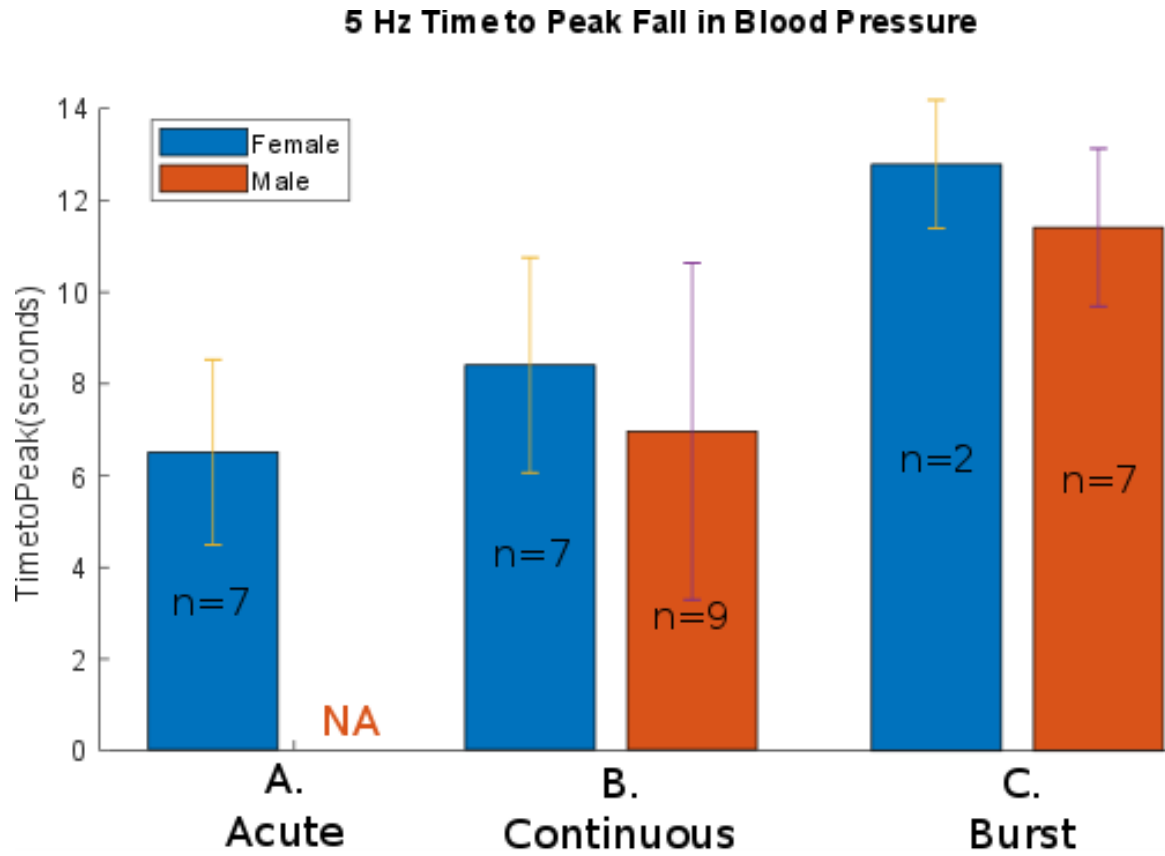


Fig. 3.8: Percent change in mean arterial pressure between baseline A and baseline B following the onset of 5 Hz stimulation differs between male and female rats. Average percent change in blood pressure (dMAP) for acute (A), continuous (B), and burst (C) paradigms. Data are means  $\pm$  SD.

### 3.4.2 Differences in Steady State Depressor and Recovery Responses: Blood Pressure

In addition to Baseline A and B, three 30-second epochs were extracted for additional analysis. The new epochs were used to quantify changes in BP and HR during sustained stimulation and shortly thereafter. Baseline X included the time before stimulation onset, baseline Y the time just prior to stimulation termination, and baseline Z 30 seconds post stimulation termination [Figure 2.7].

Using the time of stimulation onset as  $t=0$  s, the resting baseline, baseline X, is referenced at  $t = -30$  s to  $t=0$ . The baseline that marked the last 30 seconds of stimulation before termination, i.e.  $t=570$  s to  $t=600$  s, was termed baseline Y. Finally, baseline Z quantified the recovery period 30 seconds after stimulation termination, i.e.  $t=630$  s to  $t=660$  s [Figure 2.7].

The magnitude of the differences in BP within these three baselines was quantified. By finding the difference in either average blood pressure, the author compared both baseline Y and baseline Z with baseline X. Comparing baseline X with baseline Y gives an idea of the normalized % change from baseline to the new equilibrium just prior to the end of stimulation [Figure 3.9]. Conversely, comparing baseline X with baseline Z quantifies the normalized ability of BP to recover back near pre stimulation rest [Figure 3.10].

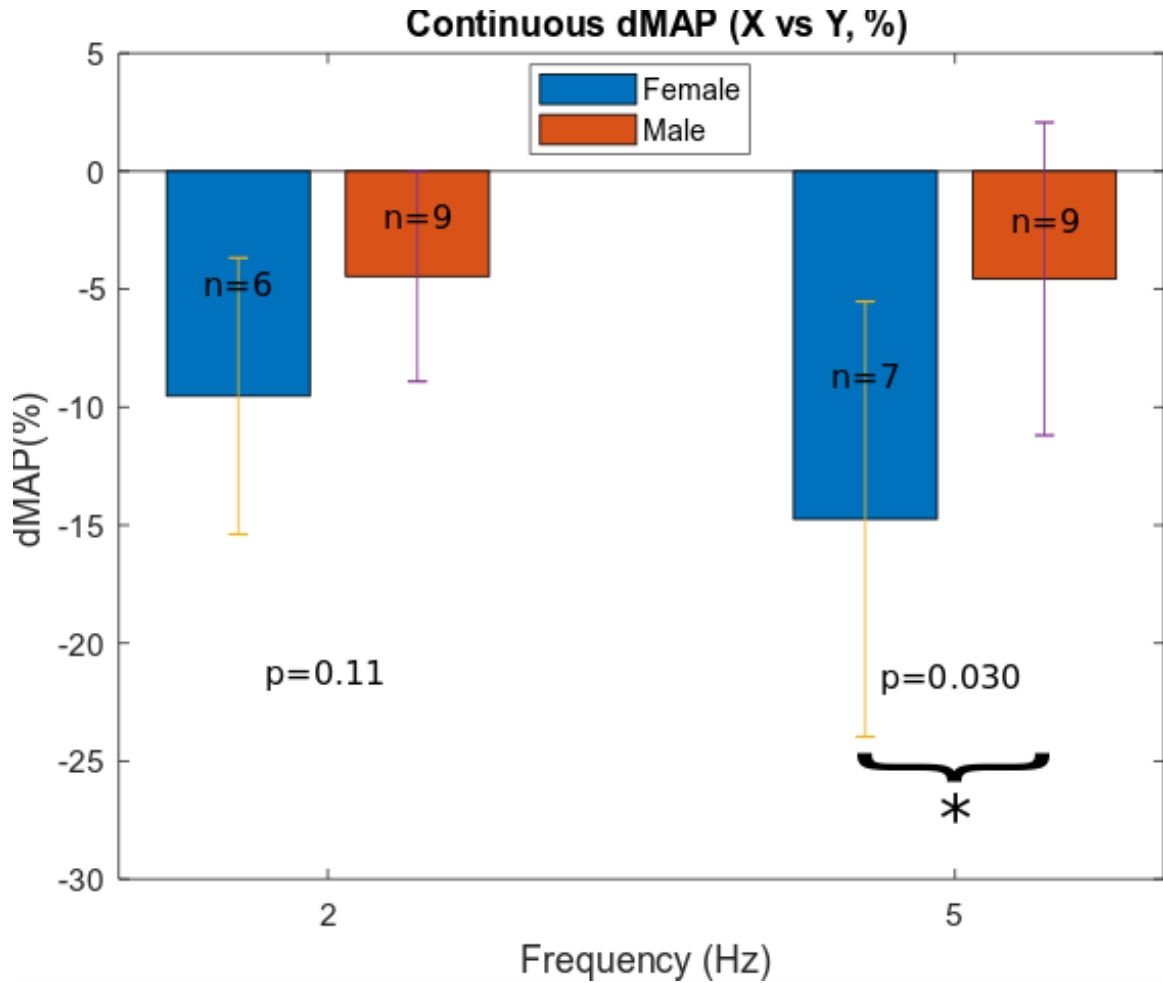


Fig. 3.9: The BRx in female rats elicits a greater residual depressor response at the end of a 600 second continuous stimulation of the left ADN than in the male rats. Average % changes in dMAP evoked through bipolar stimulation of the left ADN using randomly selected frequencies (2 and 5 Hz) at a regulated 2V amplitude.

Data are means  $\pm$  SD, \*  $p < 0.05$ .

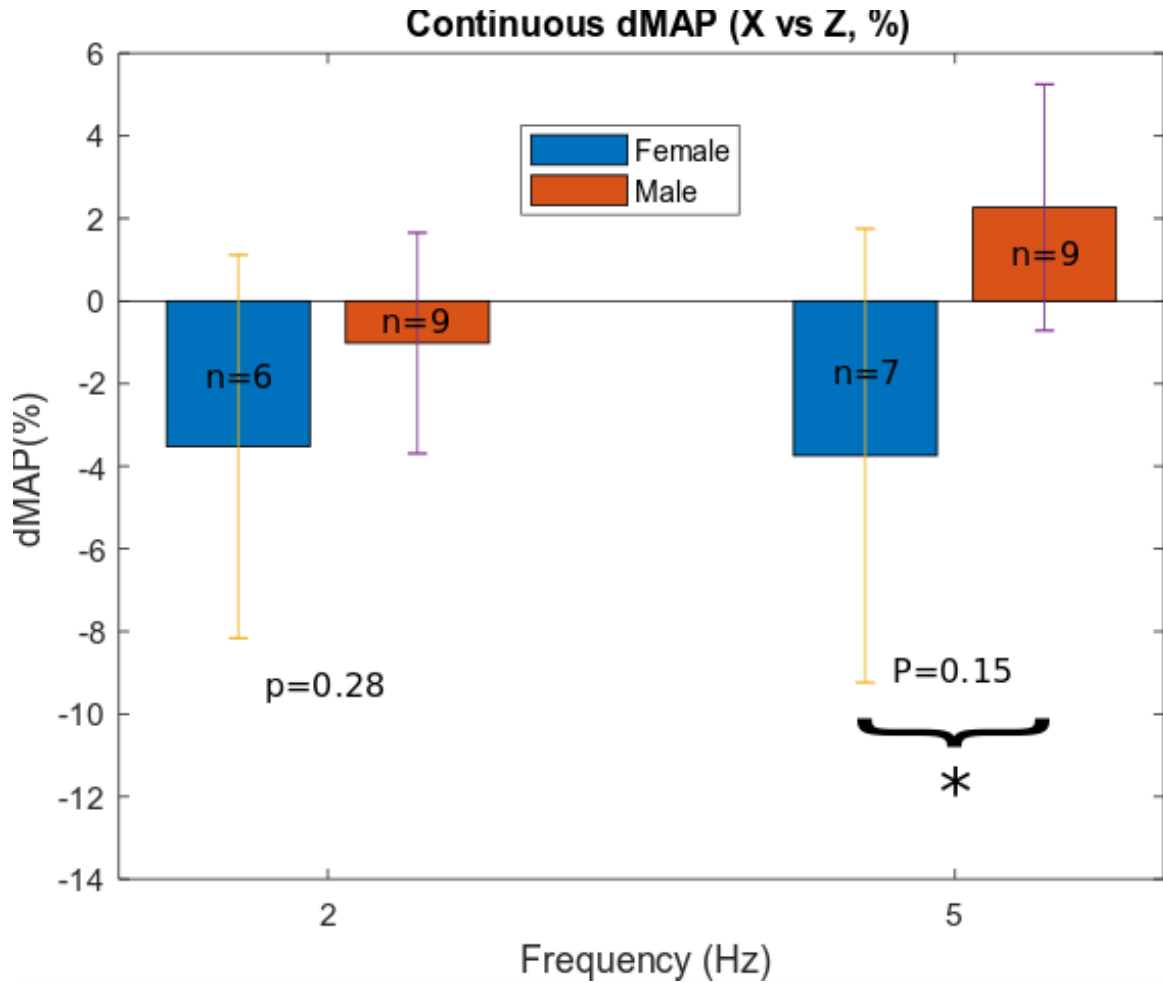


Fig. 3.10: The recovery of dMAP (baseline X vs baseline Z) following termination of continuous bipolar stimulation of the left ADN is different between male and female rats. Average % changes in dMAP evoked through bipolar stimulation of the left ADN using randomly selected frequencies (2 and 5 Hz) at a regulated 2V amplitude.

Data are means  $\pm$  SD, \*  $p < 0.05$ .

The same blood pressure analysis was carried out for the burst paradigm. Of note is the much stronger initial depressor response in the burst paradigm [Figure 3.11 3.12].

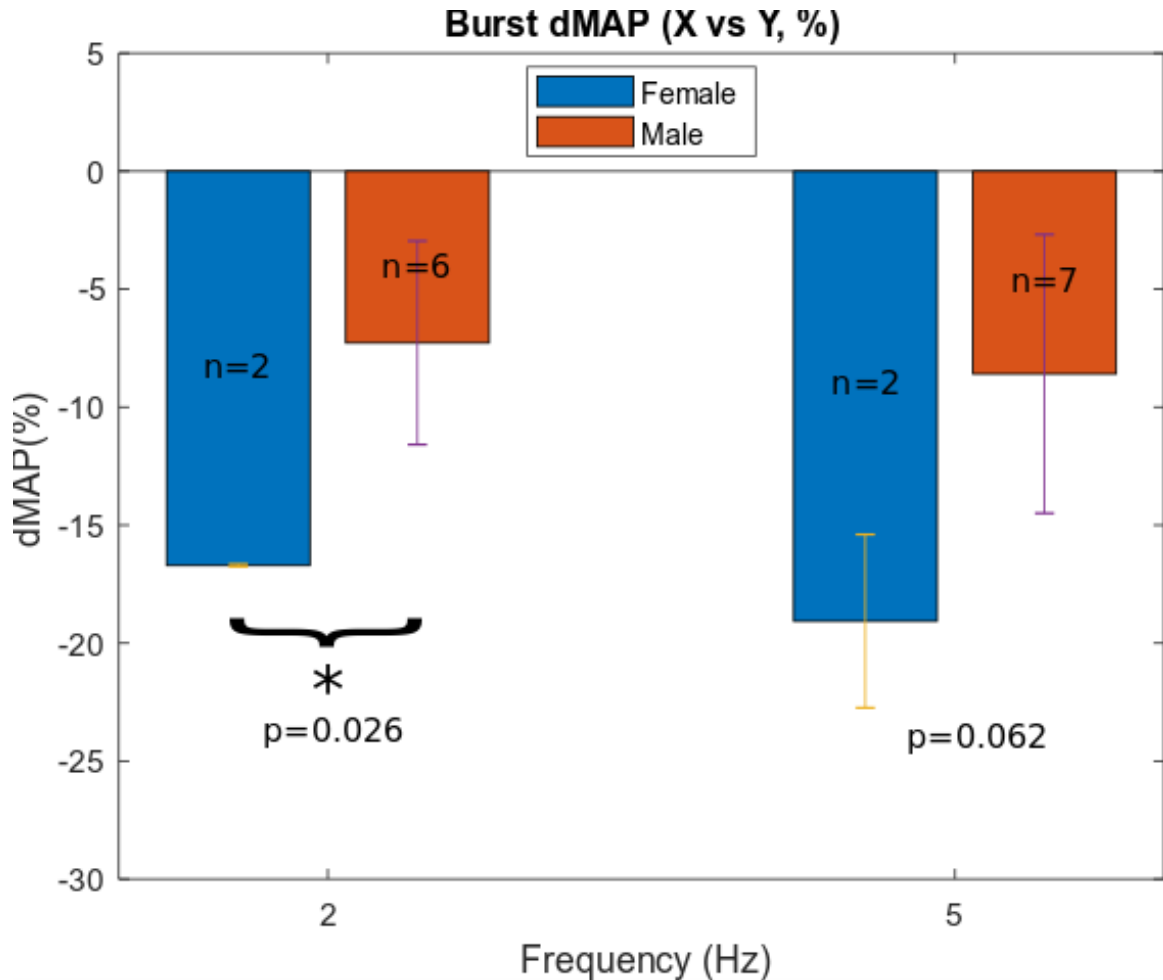


Fig. 3.11: The BRx in female rats elicits a greater depressor response at the end of a 600 second burst stimulation of the left ADN than in the male rats. Average % changes in dMAP evoked through bipolar stimulation of the left ADN using randomly selected frequencies (2 and 5 Hz) at a regulated 2V amplitude. Data are means  $\pm$  SD, \*  $p < 0.05$ .

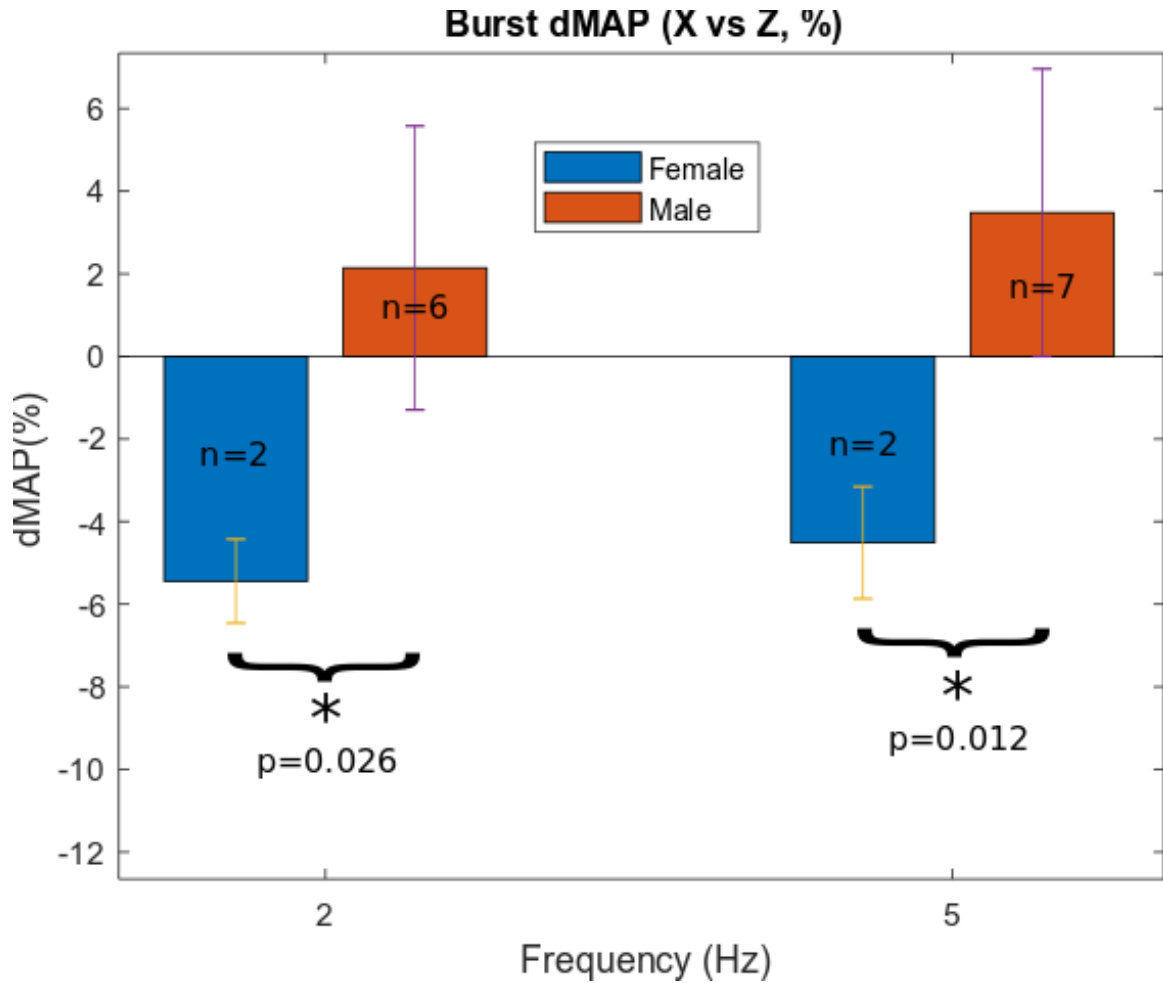


Fig. 3.12: The recovery of dMAP following termination of burst bipolar stimulation of the left ADN is different between male and female rats. Average % changes in dMAP evoked through bipolar stimulation of the left ADN using randomly selected frequencies (2 and 5 Hz) at a regulated 2V amplitude. Data are means  $\pm$  SD, \*  $p < 0.05$ .

Of additional interest was not just how the magnitude of blood pressure was returning back to baseline following the termination of stimulation, but also some insight as to the timing or speed associated with this rebound. To better quantify the speed associated with the BP returning to set point, a monoexponential fit was carried out through the fit function in MATLAB for the 10 seconds following stimulation termination. Fit type was specified as:

$$a - b * e^{-c*x} \quad (3.1)$$

And the average output for a,b, and c in each sustained paradigm were calculated for r squared values  $\geq 0.75$  [Table 3.1]. An example of an ideal exponential fit is provided [Figure 3.13].

Table 3.1: Monoexponential fit following stimulation termination: Averaged values for the variables a, b, and c as well as averaged r squared value in the 10 second monoexponential fit following termination of stimulation at t=600 seconds.

Paradigm	Sex	Freq (Hz)	n	av a	av b	av c	av $r^2$
Continuous	male	2	4	105.42	14.63	0.26	0.88
Continuous	male	5	5	107.17	14.65	0.34	0.91
Continuous	female	2	2	100.53	12.95	0.45	0.81
Continuous	female	5	4	100.84	22.50	0.36	0.83
Burst	male	2	4	105.47	17.08	0.25	0.88
Burst	male	5	7	106.47	18.14	0.26	0.92
Burst	female	2	2	94.77	13.99	0.33	0.88
Burst	female	5	1	94.73	20.14	0.31	0.87

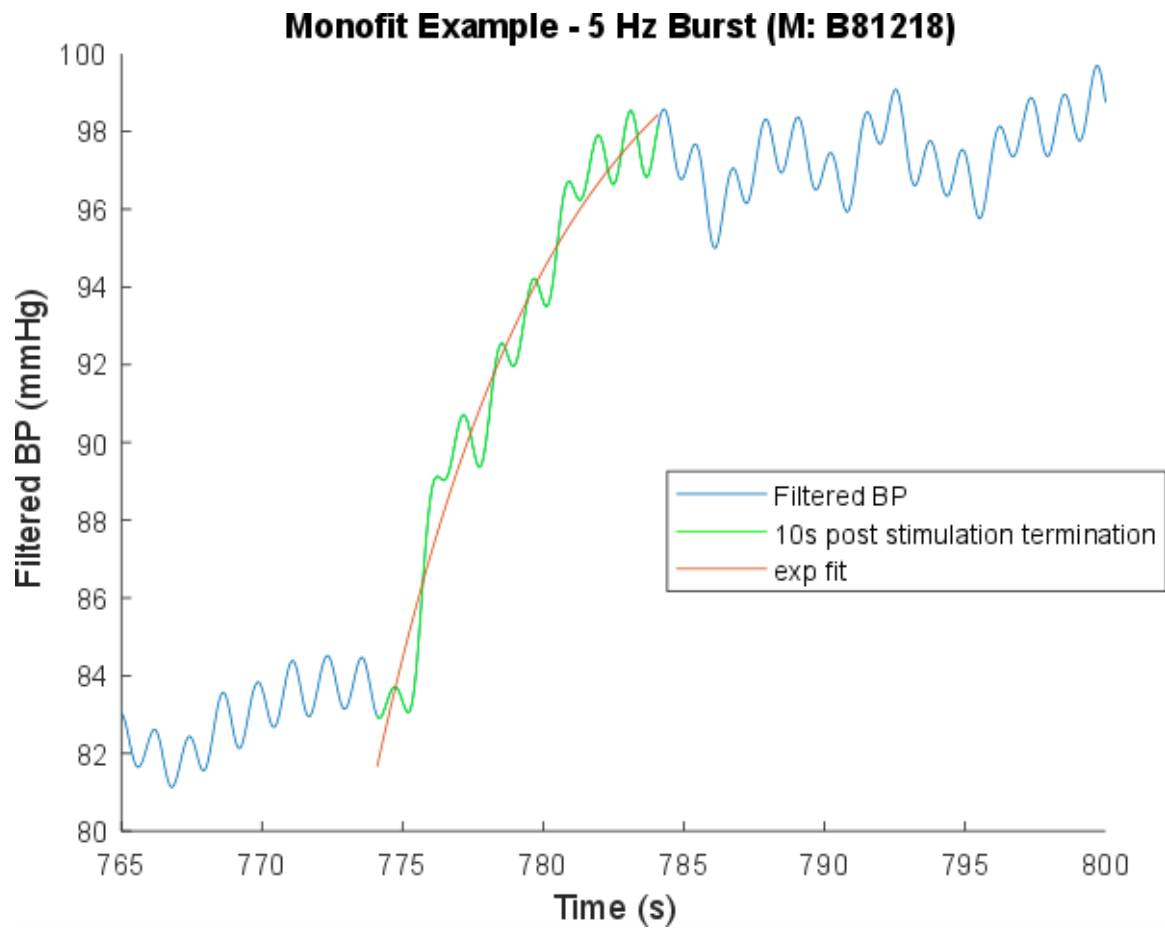


Fig. 3.13: Example of an ideal exponential fit for the 10 seconds of recovery following stimulation termination at  $t=774.34$  seconds. Filtered BP in blue, the 10 seconds of BP following stimulation termination in green, and an exponential fit with coefficients  $a=102.95$   $b=21.296$  and  $c=0.1551$  with  $r$  squared value = 0.9659.

### 3.4.3 Differences in Steady State Depressor and Recovery Responses: Heart Rate

The magnitude of the differences in HR within baselines X, Y, and Z was quantified. By finding the difference between neighboring R peaks, an estimate of beats per minute (BPM) was calculated. Changes to BPM were observed between sustained 2 Hz stimulation [Figure 3.14], sustained 5 Hz stimulation [Figure 3.15].

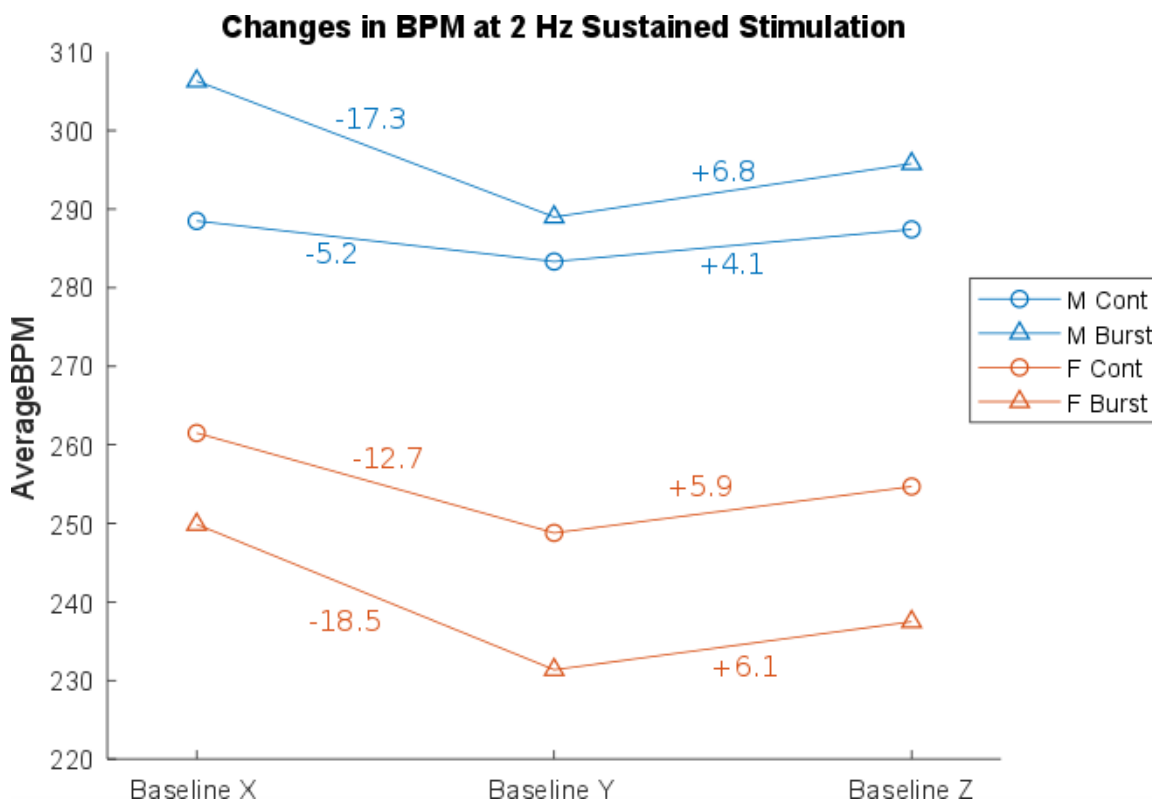


Fig. 3.14: Average change in BPM between baselines X, Y, and Z at sustained 2 Hz stimulation. Male (blue) had higher average resting BPM than female (orange). Continuous stimulation is denoted by circles and burst stimulation by triangles. Average change in BPM between baselines is denoted numerically between data points. Data are mean  $\pm$  SD.

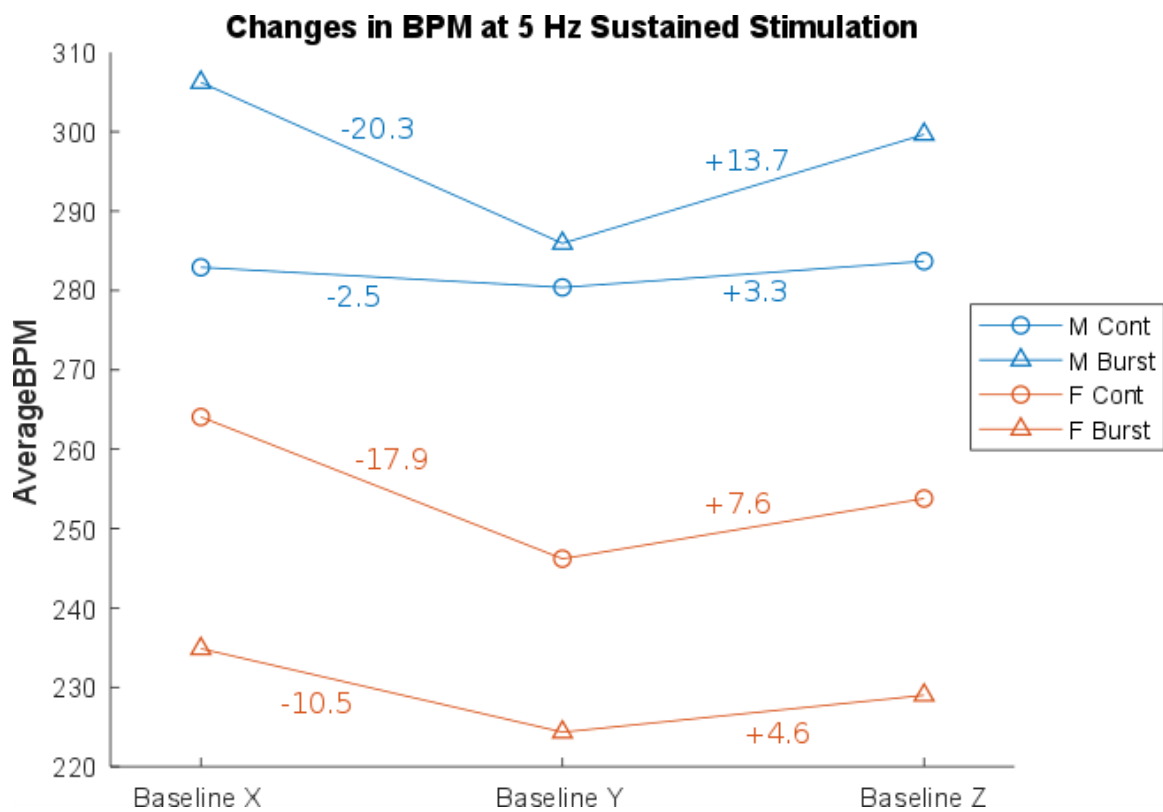


Fig. 3.15: Average change in BPM between baselines X, Y, and Z at sustained 5 Hz stimulation. Male (blue) had higher average resting BPM than female (orange). Continuous stimulation is denoted by circles and burst stimulation by triangles. Average change in BPM between baselines is denoted numerically between data points. Data are mean  $\pm$  SD.

## CHAPTER 4. DISCUSSION

### 4.1 General Conclusions

The findings from this work offer a new perspective concerning the interactions between the two divisions of the autonomic nervous system on cardiovascular homeostasis. It both confirmed previous observations of acute, robust, and repeatable sexually dimorphic parasympathetic mediated depressor response [9] and confirmed that the sexual dimorphic characteristics carried over into sustained stimulation of the left ADN. Through slight interrogation of the afferent parasympathetic pathway in rat, new insights into the rich neural control mechanisms vital for this system were uncovered. The most notable findings being: (1) continuous stimulation of low-threshold myelinated afferents in rat produce two distinct sexually-dimorphic reflexogenic responses in both heart rate and blood pressure [Figure 3.9 3.14 3.15]. (2) The recovery of sustained stimulation of low-threshold myelinated afferents in rats produce two distinct and sexually-dimorphic recovery responses [Figure 3.10 3.14 3.15]. (3) The trends observed in (1) and (2) are even more distinct given burst trains of electrical stimulation [Figures 3.11 3.12 3.143.15].

## 4.2 Specific Conclusions

Reports that first documented the frequency response characteristics of baroreceptor afferents were expanded upon [14]. The unique differences in the integrated reflex response at distinct frequencies was used as a testing platform. A standard 2V pulse magnitude was used to recruit myelinated afferents exclusively. Of interest was how the responses to these electrical trains of stimulation may influence sympathovagal efferent outflow from central neural circuits.

### 4.2.1 Aim 1

#### Responses in Blood Pressure

Earlier documented reports of sexually dimorphic depressor responses to low-voltage stimulation of the left ADN were confirmed [Figure 3.2]. Since both the experimental protocol and analysis techniques were nearly identical to those used in [9], it was of little surprise to see similar, albeit, more significant, differences in the dMAP between baselines A and B in male and female rats. The author would like to note that % dMAP in the low frequencies (1-10 Hz) of the previous report documented smaller averages than those presented here, yet the trend remains. Since the previous author did not specify with great detail the algorithms used in analysis, it is difficult to say where precisely these differences might arise. The analysis techniques used here included an automatic selection of the peak depressor response within the stimulation time range. Any automatically identified responses were later accepted or rejected by extensive visual confirmation. Visual confirmation included looking at the bigger picture of the signal by taking into account natural variations seen within the homeostatic operating range of blood pressure.

## Responses in Heart Rate

These observations of a reflexogenic and robust depressor response were further documented by looking at the changes in heart rate during these same baseline windows [Figure 3.3]. Though the responses in BPM were not as significant as those seen in BP, a trend still remains. For males, no significant variation in HR was seen in baseline B until stimulation frequencies exceeded 10 Hz. For females, a reliable change was documented as soon as 2 Hz.

A fundamental limitation of this measure is the short duration selected for baseline B. Because only a 1 second epoch is selected about the minimum depressor response, a maximum of five R peaks could be identified, resulting in an average measure of 4 RRIs. This is the best case scenario: usually seen in male where resting BPM is higher and at low frequencies where little to no change in BPM is present. For females, where a lower resting heart rate is common, a change in RRI of 40% like that seen in some 50 Hz stimulations can cause as little as three R peaks to be identified in baseline B. This limits the number of sensed RRIs and results in the average BPM in this window to be calculated using just 2 data points. This likely contributed to the large standard error seen in all measures of BPM and likely contributed to the decreased significance seen at low frequencies. BRx control on BP is rather obvious, yet effects on HR may be more complicated.

## Responses in Time to Peak Depressor Response

Acute application of electrical stimulation produce sexually dimorphic times to peak blood pressure response [Figure 3.4]. While none of these measures were statistically significant, there seemed to be some trend observed with female depressor responses requiring a longer TTP. Additional surgical experience and better fabrication of instrumentation could provide more significant trends if repeated. Tip integrity was the biggest inhibitor of reliable and repeatable results. Tip angle heavily influenced the patency of the in-line catheter, resulting in huge variations in systolic

and diastolic resolution. Not only were variations apparent in resolution, but timing between the systolic peaks and R peaks would vary animal to animal. Additionally, intermittent blockages such as vascular tissue caused dampening of spatial and temporal resolution of peaks. If better recorded, these data could provide some insight to the way in which rate-of-change encoding mechanisms at BR terminal endings is integrated at central neural structures and how it influences sympathovagal balance between males and females. To the authors knowledge, there is very little work that investigates these interactions yet it could provide a plethora of insight. Undoubtedly, this should be explored more.

#### 4.2.2 Aim 2

Results observed the sexually dimorphic aspects of acute activation of the BRx carries over into sustained applications.

#### Differences in Peak Depressor Dynamics of Baroreflex Control

The % dMAP between baselines A and B was first quantified at the 2 Hz sustained frequency [Figure 3.5]. The percent change in the peak depressor response of the continuous stimulation was almost identical to that of the acute stimulation. There still existed a statistically significant difference between males and females at 2 Hz in the continuous dMAP ( $p = 0.031$ ) but due to low number of ns for burst females, a statistically significant trend was not observed ( $p = 0.078$ ). The peak depressor response for males and females at 2 Hz in burst stimulation ( $-18.8 \pm 9.25\%$  and  $-33.9 \pm 6.04\%$ ) was far greater than in either the continuous ( $-3.84 \pm 4.57\%$  and  $-9.57 \pm 4.35\%$ ) or acute ( $-2.849 \pm 5.16 \%$  and  $-11.34 \pm 2.97 \%$ ) stimulation paradigms. The burst %d MAP for females was quite close to the 10 Hz equivalent seen in the acute paradigm,  $-33.97 \pm 6.04\%$  versus  $-40.383 \pm 11.75\%$ , respectively. The male % dMAP was higher in the burst paradigm than the acute,  $-18.78 \pm 9.25 \%$  versus  $-11.74 \pm 8.82\%$ , respectively.

A similar trend did not carry over in the 5 Hz frequency [Figure 3.6]. Interestingly, there seemed to be a much greater initial depressor response in continuous males ( $-15.225 \pm 10.25$  mmHg) than acute males ( $-4.91 \pm 7.37$  %). The burst acute (M:  $-31.13 \pm 7.71$  %; F:  $-37.18 \pm 19.93$  %) trends for males and females were similar to those observed in [Figure 3.2] and were again close to the 20 Hz (M:  $-23.09 \pm 9.68$  % and F:  $-43.14 \pm 16.43$ %) equivalent for the acute paradigms. It is unknown what may have accounted for the large depressor response in the continuous males, but a second look at the animal data showed a few outliers, of which one (B80904) had a % dMAP of  $-37.35$ %. This is well over any 5 Hz depressor response seen elsewhere, except for  $n=2$  runs in the burst protocol.

The short duration BPM comparisons at 2 and 5 Hz followed similar trends as those observed in [Figure 3.3] except for, again, the 5 Hz continuous males. This makes sense given the unique difference observed in the % dMAP at this same frequency.

In comparing short term TTP, a surprising result was the presence of a TTP for 5 Hz continuous males. Interestingly, the TTP for males in the burst paradigm at 2 Hz was slower than that in females (M:  $8.56 \pm 2.33$  sec; F:  $7.70 \pm 1.21$  sec). This is the only instance of this and could likely be due to the low  $n$  for females or femoral catheter issues discussed earlier.

### **Differences in Steady State Depression and Recovery of Blood Pressure to Sustained Stimulation**

The measure of % dMAP between baselines X and Y was used to quantify the normalized difference between the original set point and the new set point at the end of the sustained stimulation. For continuous stimulation, there was a significant difference between males and females at a frequency of 5 Hz ( $p=0.030$ ) but not at 2 Hz ( $p=0.11$ ). This trend flipped in the burst case, where a significant difference existed between males and females at 2 Hz ( $p=0.026$ ), but not quite at 5 Hz ( $p=0.062$ ).

Additional female samples of the burst protocol could aid in the significance of these data.

The measure of dMAP between baselines X and Z was used to quantify the normalized difference between the original set point and the recovery to the original set point following 30 seconds of recovery post stimulation termination. For continuous stimulation, there existed a significant difference between the recovery of BP between males and females at 5 Hz stimulation ( $p=0.015$ ) but not at 2 Hz ( $p=0.28$ ). Interestingly, the recovery in males at 5 Hz actually went past the original set point value, on average (dMAP X vs Z =  $2.28 \pm 1.02$  mmHg). For the burst paradigm, there was a significant difference between males and females in dMAP X vs Z at 2 Hz ( $p=0.026$ ) and at 5 Hz ( $p=0.012$ ). The author recommends taking these data with caution, as the ns for the female trial are low. However, the trend of males having a new baseline above the original baseline persisted to an even greater degree. In 2 Hz, the new set point was around 2 mmHg higher than that measured in baseline X while the 5 Hz case produced an almost 4 mmHg increase.

The author believes there to be two possible explanations for this phenomena. The first is an increased gain in sympathetic efferent outflow in males OR a decrease in sympathetic inhibition. The second is a decrease in the gain of parasympathetic outflow OR an increase in parasympathetic inhibition. Earlier studies suggest that, in measuring mean sympathetic nerve activity, the resting sympathetic vasomotor tone in males is higher than females, arguing for the first explanation.

Not to be overlooked, the recovery of the females seemed to never return to baseline for any of the sustained protocols. At both 2 and 5 Hz for continuous and sustained stimulation, the averages were all at least 3 mmHg below the original resting pressure. This too may point to a potential sexually dimorphic difference in central regulation of efferent outflow following sustained stimulation.

It was of additional interest how this return to baseline following stimulation termination was not just changing in overall magnitude, but also the time course which it followed. To aid in quantifying the differences, a monoexponential fit was calculated

in attempt to gain more insight. Interestingly, in all sustained paradigms, the return to baseline (variable  $c$ ) happened at a faster rate in males than in females at both 2 and 5 Hz [Table 3]. The author recommends accepting these data with caution, as the low  $n$  values and weak  $r$  squared values could certainly be improved upon. This does open the question as to what the relative differences in the gain between each division of the ANS may be playing a part in this recovery following termination. In both dMAP and in the monoexponential fit, it seems that the rate of recovery is faster in males than females. Additional curve fits should be explored with perhaps alternative fit types to better understand differences in recovery between males and females. A fundamental limitation of the method employed involved estimating starting point values. Having no precedence, the author arbitrarily chose  $a=100$ ,  $b=10$ , and  $c=0.1$  as starting point, which, while close to average values, could have played a large part in the low  $r$  squared values since  $a$  number  $a$  and  $b$  values fell outside of this range.

### **Differences in Steady State Depression and Recovery of Heart Rate to Sustained Stimulation**

The change in BPM differed considerably between sustained and burst protocols at both 2 and 5 Hz [Figure 32, 33] Of note is the strong decrease in HR between baselines X and Y especially in females. A considerable increase in BPM was seen in males following burst stimulation at 2 Hz (+6.8 BPM) and at 5 Hz (+13.7 BPM). It is important to note the large amount of error in nearly all male measures, as well as in female continuous measures. Error seemed to be a function of sample size, bringing into question the potential depth anesthesia. Since sustained trials were always the last of the paradigms to be carried out, it is possible animals were, on average, at a lower level of anesthetic depth. Potentially biasing the average BPM between animals. The difference in anesthesia depth may also explain some of the differences in resting BPM between paradigms. It is worth exploring if concentration of administered anesthetic should be dependent not only upon weight, but perhaps

upon sex and/or age. It would be worth the time to go back and attempt to correlate BPM differences with overall time of procedure, sex, and age. It came to the authors attention late in the data collection process that a smaller dose of anesthetic for females had better outcomes with respect to overall autonomic homeostasis.

### **4.3 Additional Areas to Explore**

There seems to exist an interesting inflection in both the continuous and burst paradigms in male rats that does not seem nearly as pronounced in female rats. This rainbow effect seems to negate the initial depressor response, and is often followed by a second fall in BP to a new mean. This was observed 8 of the male burst and 6 of the male sustained runs while only happening in 3 of the female runs. The female runs which exhibited this rainbow effect were only in the 5 Hz continuous paradigm, and none were observed in the burst paradigms. This may provide an additional area to explore for the sympathovagal interaction occurring during sustained stimulation, though the current experimental paradigm was not sufficient to explore this in detail.

### **4.4 Conclusion**

This work provides sufficient evidence to reject the null hypothesis. Specifically, there exists substantial significant data to support that the sexually dimorphic depressor response seen in acute paradigms carries over to the sustained paradigms. Further, this trend is compounded when sustained electrical stimulation is changed from a continuous application to a burst application.

## LIST OF REFERENCES

## LIST OF REFERENCES

- [1] E. J. Benjamin, P. Muntner, A. Alonso, M. S. Bittencourt, C. W. Callaway, A. P. Carson, A. M. Chamberlain, A. R. Chang, S. Cheng, S. R. Das, F. N. Delling, L. Djousse, M. S. Elkind, J. F. Ferguson, M. Fornage, L. C. Jordan, S. S. Khan, B. M. Kissela, K. L. Knutson, T. W. Kwan, D. T. Lackland, T. T. Lewis, J. H. Lichtman, C. T. Longenecker, M. S. Loop, P. L. Lutsey, S. S. Martin, K. Matsushita, A. E. Moran, M. E. Mussolino, M. O'Flaherty, A. Pandey, A. M. Perak, W. D. Rosamond, G. A. Roth, U. K. Sampson, G. M. Satou, E. B. Schroeder, S. H. Shah, N. L. Spartano, A. Stokes, D. L. Tirschwell, C. W. Tsao, M. P. Turakhia, L. B. VanWagner, J. T. Wilkins, S. S. Wong, and S. S. Virani, "Heart disease and stroke statistics 2014;2019 update: A report from the american heart association," *Circulation*, vol. 0, no. 0, p. CIR.0000000000000659. [Online]. Available: <https://www.ahajournals.org/doi/abs/10.1161/CIR.0000000000000659>
- [2] S. A. Patel, M. Winkel, M. K. Ali, K. M. Narayan, and N. K. Mehta, "Cardiovascular mortality associated with 5 leading risk factors: national and state preventable fractions estimated from survey data," *Ann Intern Med*, vol. 163, no. 4, pp. 245–53, 2015.
- [3] "The world health report 2012," *The World Health Organization*, vol. 2012:58.
- [4] I. Llewellyn-Smith and A. Verberne, *Central Regulation of Autonomic Functions*. Oxford University Press, 2011. [Online]. Available: <https://books.google.com/books?id=rx3py7GO7yoC>
- [5] J. Feher, *Quantitative Human Physiology: An Introduction*. Elsevier Science, 2012. [Online]. Available: <https://books.google.com/books?id=cDYMIzdJn9sC>
- [6] T. N. Thrasher, "Unloading arterial baroreceptors causes neurogenic hypertension," *Am J Physiol Regul Integr Comp Physiol*, vol. 282, no. 4, pp. R1044–53, 2002.
- [7] A. Loewy and K. Spyer, *Central Regulation of Autonomic Functions*. Oxford University Press, 1990. [Online]. Available: <https://books.google.com/books?id=Oow8w12CHwgC>
- [8] G. Mancia and G. Grassi, "The autonomic nervous system and hypertension," *Circ Res*, vol. 114, no. 11, pp. 1804–14, 2014.
- [9] J. Betts, *Anatomy and Physiology*. OpenStax College, Rice University, 2013. [Online]. Available: <https://books.google.com/books?id=st7ZvAEACAAJ>

- [10] H. R. Berthoud and W. L. Neuhuber, "Functional and chemical anatomy of the afferent vagal system," *Auton Neurosci*, vol. 85, no. 1-3, pp. 1-17, 2000.
- [11] B. H. Machado and M. J. Brody, "Role of the nucleus ambiguus in the regulation of heart rate and arterial pressure," *Hypertension*, vol. 11, no. 6 Pt 2, pp. 602-7.
- [12] T. E. Lohmeier, A. M. Barrett, and E. D. Irwin, "Prolonged activation of the baroreflex: a viable approach for the treatment of hypertension?" *Curr Hypertens Rep*, vol. 7, no. 3, pp. 193-8, 2005.
- [13] G. C. S. C. Chavez, "Functional contributions of a sex-specific population of myelinated aortic baroreceptors in rat and their changes following overiectomy," *Doctor of Philosophy Dissertation*, 2014.
- [14] A. C. Guyton, T. G. Coleman, J. Cowley, A. V., K. W. Scheel, J. Manning, R. D., and J. Norman, R. A., "Arterial pressure regulation. overriding dominance of the kidneys in long-term regulation and in hypertension," *Am J Med*, vol. 52, no. 5, pp. 584-94, 1972.
- [15] E. A. Wehrwein and M. J. Joyner, "Regulation of blood pressure by the arterial baroreflex and autonomic nervous system," *Handb Clin Neurol*, vol. 117, pp. 89-102, 2013.
- [16] W. Fan and M. C. Andresen, "Differential frequency-dependent reflex integration of myelinated and nonmyelinated rat aortic baroreceptors," *Am J Physiol*, vol. 275, no. 2 Pt 2, pp. H632-40, 1998.
- [17] D. A. Calhoun, D. Jones, S. Textor, D. C. Goff, T. P. Murphy, R. D. Toto, A. White, W. C.ushman, W. White, D. Sica, K. Ferdinand, T. D. Giles, B. Falkner, and R. M. Carey, "Resistant hypertension: Diagnosis, evaluation, and treatment," *Circulation*, vol. 117, no. 25, pp. e510-e526, 2008. [Online]. Available: <https://www.ahajournals.org/doi/abs/10.1161/CIRCULATIONAHA.108.189141>
- [18] S. Mendis, P. Puska, B. Norrving, W. H. Organization, W. H. Federation, and W. S. Organization, *Global Atlas on Cardiovascular Disease Prevention and Control*. World Health Organization in collaboration with the World Heart Federation and the World Stroke Organization, 2011. [Online]. Available: <https://books.google.com/books?id=ZRbKygAACAAJ>
- [19] F. Biering-Sorensen, T. Biering-Sorensen, N. Liu, L. Malmqvist, J. M. Wecht, and A. Krassioukov, "Alterations in cardiac autonomic control in spinal cord injury," *Auton Neurosci*, vol. 209, pp. 4-18, 2018.
- [20] G. A. Roth, C. O. Johnson, K. H. Abate, F. Abd-Allah, M. Ahmed, K. Alam, T. Alam, N. Alvis-Guzman, H. Ansari, J. Arnlov, T. M. Atey, A. Awasthi, T. Awoke, A. Barac, T. Barnighausen, N. Bedi, D. Bennett, I. Bensenor, S. Bidgilign, C. Castaneda-Orjuela, F. Catala-Lopez, K. Davletov, S. Dharmaratne, E. L. Ding, M. Dubey, E. J. A. Faraon, T. Farid, M. S. Farvid, V. Feigin, J. Fernandes, J. Frostad, A. Gebru, J. M. Geleijnse, P. N. Gona, M. Griswold, G. B. Hailu, G. J. Hankey, H. Y. Hassen, R. Havmoeller, S. Hay *et al.*, "The burden of cardiovascular diseases among us states, 1990-2016," *JAMA Cardiol*, vol. 3, no. 5, pp. 375-389, 2018.

- [21] J. H. Schild and D. L. Kunze, "Differential distribution of voltage-gated channels in myelinated and unmyelinated baroreceptor afferents," *Auton Neurosci*, vol. 172, no. 1-2, pp. 4–12, 2012.
- [22] P. G. Katona, J. W. Poitras, N. Pantelakis, E. W. Jensen, and G. O. Barnett, "Deterministic nature of baroreceptor firing," *Am J Physiol*, vol. 215, no. 1, pp. 1–7, 1968.
- [23] B. Fing, "Electrical and mechanical behaviors of rat aortic baroreceptors," *Doctor of Philosophy Dissertation*, 2008.
- [24] H. R. Kirchheim, *Systemic arterial baroreceptor reflexes*, 1976.
- [25] G. C. Santa Cruz Chavez, B.-Y. Li, P. A. Glazebrook, D. L. Kunze, and J. H. Schild, "An afferent explanation for sexual dimorphism in the aortic baroreflex of rat," *American journal of physiology. Heart and circulatory physiology*, vol. 307, no. 6, pp. H910–H921, 2014. [Online]. Available: <https://www.ncbi.nlm.nih.gov/pubmed/25038145>  
<https://www.ncbi.nlm.nih.gov/pmc/PMC4166749/>
- [26] J. L. Seagard, J. F. van Brederode, C. Dean, F. A. Hopp, L. A. Gallenberg, and J. P. Kampine, "Firing characteristics of single-fiber carotid sinus baroreceptors," *Circ Res*, vol. 66, no. 6, pp. 1499–509, 1990.
- [27] P. Thoren and J. V. Jones, "Characteristics of aortic baroreceptor c-fibres in the rabbit," *Acta Physiol Scand*, vol. 99, no. 4, pp. 448–56, 1977.
- [28] M. Andresen and J. F. R. Paton, *The Nucleus of the Solitary Tract: Processing Information from Viscerosensory Afferents*, 2011.
- [29] M. Chapleau, G. Hajduczuk, and F. M. Abboud, *Peripheral and central mechanisms of baroreflex resetting*, 1989, vol. 15.
- [30] P. A. Munch, M. C. Andresen, and A. M. Brown, "Rapid resetting of aortic baroreceptors in vitro," *Am J Physiol*, vol. 244, no. 5, pp. H672–80, 1983.
- [31] C. M. Heesch and K. W. Barron, "Is there a central nervous system component to acute baroreflex resetting in rats?" *Am J Physiol*, vol. 262, no. 2 Pt 2, pp. H503–10, 1992.
- [32] E. M. Hagen, "Acute complications of spinal cord injuries," *World journal of orthopedics*, vol. 6, no. 1, pp. 17–23, 2015. [Online]. Available: <https://www.ncbi.nlm.nih.gov/pubmed/25621207>  
<https://www.ncbi.nlm.nih.gov/pmc/PMC4303786/>
- [33] A. A. Phillips, A. V. Krassioukov, P. N. Ainslie, and D. E. Warburton, "Baroreflex function after spinal cord injury," *J Neurotrauma*, vol. 29, no. 15, pp. 2431–45, 2012.
- [34] N. McCarty and B. Silverman, "Cardiovascular autonomic neuropathy," in *Baylor University Medical Center Proceedings*, vol. 29. Taylor and Francis, Conference Proceedings, pp. 157–159.

- [35] C. A. Swenne, “Baroreflex sensitivity: mechanisms and measurement,” *Netherlands heart journal : monthly journal of the Netherlands Society of Cardiology and the Netherlands Heart Foundation*, vol. 21, no. 2, pp. 58–60, 2013. [Online]. Available: <https://www.ncbi.nlm.nih.gov/pubmed/23179611>  
<https://www.ncbi.nlm.nih.gov/pmc/PMC3547418/>
- [36] M. Wallbach and M. J. Koziolk, “Baroreceptors in the carotid and hypertensionssystematic review and meta-analysis of the effects of baroreflex activation therapy on blood pressure,” *Nephrology Dialysis Transplantation*, vol. 33, no. 9, pp. 1485–1493, 2017. [Online]. Available: <https://doi.org/10.1093/ndt/gfx279>
- [37] I. J. M. Scheffers, A. A. Kroon, J. Schmidli, J. Jordan, J. J. M. Tordoir, M. G. Mohaupt, F. C. Luft, H. Haller, J. Menne, S. Engeli, J. Ceral, S. Eckert, A. Erglis, K. Narkiewicz, T. Philipp, and P. W. de Leeuw, “Novel baroreflex activation therapy in resistant hypertension: Results of a european multi-center feasibility study,” *Journal of the American College of Cardiology*, vol. 56, no. 15, pp. 1254–1258, 2010. [Online]. Available: <http://www.sciencedirect.com/science/article/pii/S0735109710027221>